

Imperial College London

Department of Electrical and Electronic Engineering

Final Year Project Report 2017



Project Title: **Design and Evaluation of a Series Active Variable Geometry Suspension for use in a Sports Car**

Student: **Andrew Zhou**

CID: **00938859**

Course: **EEE3**

Project Supervisor: **Dr Simos Evangelou**

Second Marker: **Dr Imad Jaimoukha**

Abstract

This project aims to design and subsequently simulate and evaluate the performance of a Series Active Variable Geometry Suspension (SAVGS) for use in a sports car. Work has been carried out to obtain the physical parameters of the MX5 and to design a controller before the SAVGS performance was simulated and evaluated.

SAVGS, a lightweight and reliable solution for improving the comfort and handling of a car, consists of mechanical elements and a controller, which must be designed with consideration to the unique parameters of this project's object of study, the Mazda MX5. Many of the required parameters of the car are unavailable from first party sources such as the MX5's user handbook, so estimations were made either using third party data from car owners or by carrying out informed calculations. The controller in particular must take into account the parameters of both the car and the SAVGS, and will be connected in a closed loop with a linearised model of the car suspension. The H_∞ control method was chosen over the Proportional Integral Derivative (PID) and μ -synthesis methods to synthesise the controller, due to its simplicity and proven performance. The behaviour of the car when retrofitted with SAVGS and subjected to road disturbances was simulated utilising an AutoSim model in conjunction with Simulink and MATLAB toolboxes. The performance of the active suspension was evaluated by drawing a comparison with the MX5's standard passive suspension under identical conditions, and quantified using industry standard methods. Results demonstrate that the SAVGS generally outperformed the passive suspension in both comfort and handling metrics, and was less power demanding than typical active suspensions.

The outcomes of this project will provide suspension designers with valuable data that is expected to aid the automotive industry in advancing car suspension technologies.

Contents

| | |
|--|------------|
| Abstract | i |
| List of Tables | vii |
| List of Figures | ix |
| List of Abbreviations | xi |
| 1 Introduction | 1 |
| 1.1 Series Active Variable Geometry Suspension | 1 |
| 1.2 Project Objectives and Methodology | 2 |
| 1.3 Report Outline | 3 |
| 2 Background | 4 |
| 2.1 Purpose of the Suspension System | 4 |
| 2.2 Suspension Construction and Physics | 5 |
| 2.3 Suspension Designs | 7 |
| 2.3.1 Passive | 7 |

| | | |
|-------|---|----|
| 2.3.2 | Active | 8 |
| 2.3.3 | Semi-active | 9 |
| 2.3.4 | Series Active Variable Geometry Suspension | 9 |
| 2.4 | Road Disturbances and Sensitivity on the Human Body | 10 |
| 2.4.1 | Road Quality Classification | 11 |
| 2.4.2 | Human Sensitivity to Vibration | 11 |
| 2.4.3 | Performance Metrics for Road Isolation and Road Holding | 12 |
| 2.5 | Car and Suspension Modelling | 13 |
| 2.5.1 | Quarter Car Model Concept and Theory | 13 |
| 2.5.2 | Half Car Model Concept and Theory | 14 |
| 2.5.3 | Full Car Model Concept and Theory | 14 |
| 2.5.4 | Multi-body Car Model for Simulation | 15 |
| 2.6 | Controller Methodology Controller and Selection | 15 |
| 2.6.1 | PID Control | 16 |
| 2.6.2 | Robust Linear Control | 16 |
| 2.6.3 | H_∞ Control | 17 |
| 2.6.4 | μ -synthesis Control | 17 |
| 2.7 | Software | 17 |
| 2.8 | Background Summary and Conclusions | 18 |

| | | |
|----------|---|-----------|
| 3 | Sports Car Suspension Modelling | 19 |
| 3.1 | Sports car vs GT car | 19 |
| 3.2 | Motivation Behind Car Selection | 20 |
| 3.3 | Simulation Model Modifications for the MX5 | 21 |
| 3.3.1 | SAVGS Linearised Model | 21 |
| 3.3.2 | SAVGS State Space Model | 24 |
| 3.4 | MX5 Physical Parameters | 27 |
| 3.5 | Chapter Summary and Conclusions | 30 |
| 4 | SAVGS and Controller Design for the MX5 | 31 |
| 4.1 | SAVGS Mechanics | 31 |
| 4.1.1 | Single Link Motor and Gearbox | 31 |
| 4.1.2 | Single Link Length Considerations for the MX5 | 32 |
| 4.2 | Controller Inputs and Outputs | 34 |
| 4.2.1 | Exogenous Disturbances, w | 34 |
| 4.2.2 | Control objectives and constraints, z | 35 |
| 4.2.3 | Measurements, y | 35 |
| 4.2.4 | Control action, u | 36 |
| 4.3 | System Interconnection | 36 |
| 4.4 | Chapter Summary and Conclusions | 39 |

| | | |
|----------|--|-----------|
| 5 | Simulation Results and Analysis | 40 |
| 5.1 | Quarter Car Simulations | 40 |
| 5.1.1 | Quarter Car Simulation Results on a Single Bump | 41 |
| 5.1.2 | Quarter Car Simulation Results on a Random Road Profiles | 43 |
| 5.2 | Full Car Simulations | 47 |
| 5.2.1 | Full Car Simulation Results on a Single Bump | 47 |
| 5.2.2 | Full Car Simulation Results on Random Road Profiles | 48 |
| 5.3 | Chapter Summary and Conclusions | 50 |
| 6 | Conclusions and Future Work | 52 |
| 6.1 | Future Work | 53 |
| | Bibliography | 54 |

List of Tables

| | | |
|-----|---|----|
| 3.1 | Hand Derived Model Parameters | 22 |
| 3.2 | MX5 Parameters | 28 |
| 5.1 | Summary of improvements for quarter car on a bump | 43 |
| 5.2 | Summary of Road Class Values | 44 |
| 5.3 | Summary of improvements for Class A road | 46 |
| 5.4 | Summary of improvements for Class C road | 47 |
| 5.5 | Summary of improvements for full car on a bump | 48 |

List of Figures

| | | |
|-----|--|----|
| 2.1 | Simplest version of SAVGS. (a) and (b) are different configurations that can be achieved by applying torque about G [12] | 9 |
| 2.2 | Displacement of power spectral density, G_d , as a function of spatial frequency n . [12]. Roads A, B and C are considered good, average and poor roads [19] | 11 |
| 2.3 | Quarter Car Mathematical Model [20] | 13 |
| 2.4 | Half Car Mathematical Model [20] | 14 |
| 2.5 | Full Car Mathematical Model [20] | 15 |
| 3.1 | Left: Passive double-wishbone suspension. Right: SAVGS retrofitted double-wishbone suspension [1] | 20 |
| 3.2 | Linear model without strong dependency on SL angle [12] | 21 |
| 3.3 | Left: SAVGS Retrofitted onto a double-wishbone suspension. Right: Hand-derived model [12] | 22 |
| 3.4 | The evolution of α with single link angle for the front of the MX5 | 23 |
| 3.5 | Evolution of β with single link angle for the front of MX5 | 24 |
| 4.1 | Graph of SAVGS torque against vertical tyre force increment for different SL arm lengths options for the front wheel with standard spring stiffness [34] | 33 |

| | | |
|-----|---|----|
| 4.2 | Graph of SAVGS torque against vertical tyre force increment for different SL arm lengths options for the rear wheel with standard spring stiffness [34] | 33 |
| 4.3 | System interconnection [1] | 37 |
| 4.4 | Bode plots of the comfort and handling targets | 39 |
| 5.1 | Left: Sprung mass acceleration. Right: Tyre deflection for front quarter car . . . | 42 |
| 5.2 | Left: Sprung mass acceleration. Right: Tyre deflection for rear quarter car . . . | 42 |
| 5.3 | PSD of Left: Sprung mass acceleration. Right: Tyre deflection for front quarter car on a class A road | 45 |
| 5.4 | PSD of Left: Sprung mass acceleration. Right: Tyre deflection for rear quarter car on a class A road | 45 |
| 5.5 | PSD of Left: Sprung mass acceleration. Right: Tyre deflection for front quarter car on a class C road | 46 |
| 5.6 | PSD of Left: Sprung mass acceleration. Right: Tyre deflection for rear quarter car on a class C road | 46 |
| 5.7 | Left: Sprung mass acceleration of centre of gravity of full car. Right: Tyre deflection for front left tyre of full car. | 48 |
| 5.8 | Left: PSD of Sprung mass acceleration of centre of gravity of full car. Right: PSD of average Tyre deflection of full car for a class A road. | 49 |
| 5.9 | Left: PSD of Sprung mass acceleration of centre of gravity of full car. Right: PSD of Tyre deflection for front left tyre of full car for a class C road. | 50 |

List of Abbreviations

| | |
|-------|--|
| AVGS | Active Variable Geometry Suspension |
| dB | Decibels |
| DOF | Degree of Freedom |
| GT | Grand Tourer |
| ISO | International Organisation for Standardisation |
| LW | Lower Wishbone |
| PSD | Power Spectral Density |
| QC | Quarter Car |
| SAVGS | Series Active Variable Geometry Suspension |
| SD | Spring Damper |
| SL | Single Link |
| UW | Upper Wishbone |

Chapter 1

Introduction

1.1 Series Active Variable Geometry Suspension

The main purposes of the suspension system in a car are to improve ride comfort for passengers, and to allow the tyres to maintain contact with the road to improve handling. This is done by controlling the vertical motion of the car body and tyres. Suspension systems can be categorised as either passive, semi-active or active suspensions depending on how they achieve this control.

Passive suspension systems are purely mechanical solutions featuring a spring-damper unit, and typically cause the ride comfort and car handling to work at odds, forcing the car designer to make a compromise. Semi-active and active suspensions implement an electrical element to enable the use of control techniques to improve upon the performance of the passive suspension. Active suspensions offer the best performance, with many different designs currently being employed in the industry including hydraulic and pneumatic solutions. The drawbacks of these suspension systems are their high power consumption, inability to function in case of power loss, increased mass, and cost. These factors stop active suspensions from being widely used.

Series Active Variable Geometry Suspension (SAVGS), is a relatively new solution that aims to avoid the problems of existing active suspensions, whilst still offering improved performance over passive and semi-active suspensions. Significant groundwork has been laid out on the concept

of SAVGS and its benefits when retrofitted onto a Grand Tourer (GT) car, specifically a Ferrari F430. The aim of this project is to evaluate the performance of SAVGS when retrofitted onto a sports car, namely the Mazda MX5, via computer simulation. This will be done by modifying existing simulation models made for the GT car by changing appropriate parameters.

Aside from the parameter differences, the two cars will be designed for different purposes, and thus their suspensions must be tuned towards different tasks. The F430 is a high end performance vehicle that will have a suspension system that strives towards track performance, whilst the sports car is more modestly priced and will have a more balanced suspension for people using the car for every day driving. The controller for the SAVGS designed for the GT car will therefore be modified when applied to the sports car in order to allow the car to stay true to its intended purpose.

If research finds that SAVGS is in reality as effective theorised, it could be widely adopted within the motor industry, as it could greatly benefit drivers and passengers alike not only in terms of ride comfort, but also in handling of the car which has implications on safety and track performance

1.2 Project Objectives and Methodology

The main aim of this project is to evaluate the performance of a retrofitted SAVGS on a sports car. It includes the following objectives:

- To acquire or estimate the parameters of the sports car to be studied
- To modify the SAVGS to best fit the vehicle's parameters
- To synthesise a controller for this modified SAVGS
- To simulate the performance of the passive and SAVGS enabled cars
- To analyse and evaluate the performance of the SAVGS against the standard passive suspension by using industry standard comfort and handling metrics

The sports car chosen to be the object of study in this project is the Mazda MX5. The controller will be synthesised based on H_∞ control theory and using MATLAB toolboxes. This software will further be used to carry out the simulations of the passive and SAVGS enabled cars with integration from Simulink and AutoSim.

1.3 Report Outline

Following on from the Introduction, this report contains 5 other chapters. Chapter 2 gives background on the purposes and different variations of suspension systems and how they are modelled. It also provides a literature review on the theory and motivation behind Series Active Variable Geometry Suspension and how its performance were evaluated.

Chapter 3 highlights the key differences between the sports car and the GT car used in previous SAVGS projects. This chapter also documents the parameters of the sports car on which the SAVGS will be retrofitted for this project, and how the old car models must be modified to accurately represent the sports car.

Chapter 4 presents the mechanics and the design of the control scheme for the SAVGS. This includes the physical components and devices needed to operate the suspension, and the theory behind the controller synthesis and interconnection.

Chapter 5 documents the simulations carried out on the SAVGS and passive. Comparisons of results between the two suspensions were also performed in this chapter.

Chapter 6 concludes the report by summarising the results and giving suggestions to future work that can be done to further investigate and improve SAVGS.

Chapter 2

Background

This chapter provides background knowledge of vehicle suspension systems and reviews the methods which have been adopted to model and evaluate the performance of the suspensions.

2.1 Purpose of the Suspension System

The suspension in a car is the system with which the body of the car is connected to the wheels to allow relative motion between the two. The purpose of the suspension is to achieve two principle functions: road isolation and road holding [1].

Road isolation is the ability of the suspension system to absorb or isolate road shock, caused by irregularities in the road such as bumps or pot holes, from the passenger compartment. Road isolation is also known as ride comfort or ride quality, as a car with good road isolation will be perceived by passengers as having a smooth, comfortable, or high quality ride.

Road holding, or handling, is the degree to which the vehicle's tyres maintain contact with the road surface when subjected to irregularities. Without tyre contact, there is no friction between the car and the road, and no traction, meaning the driver has no control over acceleration, braking or steering. This has major implications on safety and performance on a race track[2].

The suspension system also works to level the car and provide traction when the weight of the

car shifts, for example during cornering. When the car moves in a curved path, the centrifugal force causes the centre of gravity of the car to be pushed towards the outside of the curve, tipping the car across the x-axis of the chassis. This is known as body roll, and in extreme circumstances, can cause tyres to lose contact with the road[2]. To achieve road holding, the suspension system works to level the car by transferring weight from the side being lowered to the side being raised. The suspension system also transfers weight from the rear to the front during acceleration, in order to prevent "squat", and vice versa during braking to prevent "dive" [3].

As road isolation and road holding are normally at odds with each other, car manufacturers will tune their suspension systems depending on the purpose of the car. For example, a race car will typically compromise ride isolation in favour of better road handling, whereas a luxury car will favour ride quality.

2.2 Suspension Construction and Physics

The main elements of a suspension system are springs and dampers, also known as shock absorbers. Together these two components form the strut. When the vehicle gains speed, the springs are subjected to irregularities on the surface of the road. These irregularities are typically only vertical disturbances, such as bumps or pot holes, which raise or drop the height of the road, causing the spring in the suspension to compress or extend respectively. This would decrease or increase the distance between the wheel and the body of the car, keeping the body of the car level, meaning the passengers will not feel the disturbance and thus achieving road isolation. Road holding is achieved when the springs return to their equilibrium position in order to make contact with the road and provide traction after the irregularity [1].

Many different types of springs that have been used over the years by car manufacturers, including leaf springs [4] and torsion beams [5], but all work under the principle of Hooke's law. This states that the force, F , applied in the extension or compression of a spring by a distance X , is proportional to the distance:

$$F = kX$$

where k is the stiffness of the spring. Stiffness is the extent to which to which an object resists its deformation, and in a spring this would be extension or compression [6]. A stiffer spring is generally used in performance cars as they extend and regain contact with the road more quickly, providing traction and henceforth road holding. Luxury cars built for comfort feature loosely sprung suspensions that are capable of absorbing bumps in the road and smoothing the ride.

Work is done to compress or extend a spring, and doing so stores elastic potential energy. If the spring is undamped, it will continue on to oscillate at its natural frequency until all energy that was initially put in is dissipated. On a rough road surface, the violent extension of the springs would cause the car to bounce uncontrollably, so shock absorbers, or dampers, are introduced to dampen the oscillations [1]. These work by converting the suspension movement's kinetic energy into heat, which is then dissipated through some hydraulic fluid.

The road isolation versus road holding ability of the car is also affected by the unsprung to sprung mass ratios. The sprung mass of the vehicle is the mass of the car that is supported by the suspension, such as the chassis, the engine, and even passengers. The unsprung mass includes the mass of the suspension, wheels, and tyres. When a car is driven over bumps on the road, the tyre compresses, inducing a force on the unsprung mass. This force is reciprocated with a movement of the unsprung mass itself that is inversely proportional to its weight. A lighter unsprung mass can therefore respond to disturbances in the road more quickly, providing more road holding by tracking over the imperfections on the road. Thus sports cars are typically designed to have as little unsprung mass as possible, and therefore a lower unsprung to sprung mass ratio.

2.3 Suspension Designs

In general, suspensions can be categorised into either dependent or independent suspensions. Dependent suspensions rigidly link two wheels of the same axle such that a force acting on one wheel will also affect the opposite. This allows the suspension to withstand greater shock and is employed mainly in heavy vehicles.

GT and sports cars typically feature independent suspensions, which are constructed in such a way that each wheel can move independently to each other. The wheels are therefore not required to be perpendicular to a flat road surface. The angle that is formed by the wheel and road is known as the camber angle. If the top of the wheel is further from the chassis than the bottom then it is of positive camber. The opposite is known as negative camber. An example of an independent suspension that does not allow vertical movement without some degree of camber angle change is the MacPherson strut, and an example of an independent suspension that keeps camber angle constant is the double-wishbone suspension.

Suspensions can also be categorised by the methodology in which their spring motion is controlled. This is the main differentiator between SAVGS and classic passive, active, and semi-active suspensions.

2.3.1 Passive

Passive suspensions are purely mechanical solutions, offering two degrees of freedom in its design: the stiffness of the spring and the damper coefficient. These parameters are fixed and so passive suspensions are tuned solely for the intended purpose of the car. For example, if a race car was designed with a passive suspension, the spring and damper parameters will be optimised towards handling rather than comfort. The opposite would apply for a luxury car. The limitations of passive suspensions therefore come from the issue that they cannot adapt to variables such as road conditions, surfaces and speeds. However, passive suspensions have the advantages of being low weight, low cost, simple in construction and reliable [7]. Most car

manufacturers believe that for a road car, the pros of the passive suspension outweigh the cons, and are thus the most common suspension type.

2.3.2 Active

Active suspensions control the vertical movement of the wheels relative to the body of the vehicle with an on-board control system. Where the passive suspension is purely mechanical, this is an electro-mechanical solution as sensors and actuators are used in place of the spring and damper. The sensors continuously monitor body movement and vehicle ride level, and feed them into an on-board computer. Control techniques such as the "sky-hook" technique are then used to determine what action should be undertaken by the actuators, either raising or lowering the chassis at each wheel to optimise the ride. This technique offers significant improvement over passive suspensions in terms of road isolation and holding, effectively eliminating body roll in situations such as accelerating, decelerating and cornering. In addition to this, many active suspension are adjustable, meaning the driver can choose between having a softer suspension for comfort, or a harder suspension for improved road handling.

The trade-off for this is that the extra weight of the sensors and actuators decrease performance in terms of speed, acceleration, and fuel efficiency [8]. Efficiency will also be hampered by the extra power that is required to operate the actuators. Additionally, the sensors and actuator will not work in the case of power loss. A premium must also be paid to have the active suspension and its components installed onto the car, on top of increased maintenance costs. As a result active suspensions are generally only seen in high end luxury cars.

Active suspensions can also be classified according to their control bandwidth. The control bandwidth is the difference between the upper and lower frequencies of the frequency components in the control signal. A higher bandwidth means the controller has higher frequency components that can more rapidly react to input signals and formulate the necessary output. If the control bandwidth of the suspension is below the wheel hop frequency (typically 12-15Hz) then it is classified as a slow active suspension. Fast active suspensions are those with bandwidths generally ranging up to 50Hz [7]. High bandwidth suspensions are however more power

demanding and complex, leading to many manufacturers preferring slow-active suspensions.

2.3.3 Semi-active

A semi-active suspension is similar to a passive suspension in that it uses springs and dampers, but unlike a passive suspension, the damping coefficient of the damper is variable, and changes the characteristics of the suspension. The most common type of semi-active suspension is solenoid/valve actuated, which consists of a solenoid valve which varies the opening section of the shock absorber, controlling the flow of the hydraulic fluid and therefore altering the damping characteristics [9]. The opening of the valve is typically controlled by a magnetic field induced by an external current. Semi-active suspensions therefore do not require power to operate and the suspension will be effectively passive in case of power loss.

With a proper control strategy, semi-active suspensions achieve greater ride comfort and road handling than passive suspensions [10], but to a lesser extent than active suspensions [11].

2.3.4 Series Active Variable Geometry Suspension

Series Active Variable Geometry Suspension aims to improve upon the ride quality and handling offered by passive and semi-active suspensions, whilst avoiding the main disadvantages of typical active suspensions [12].

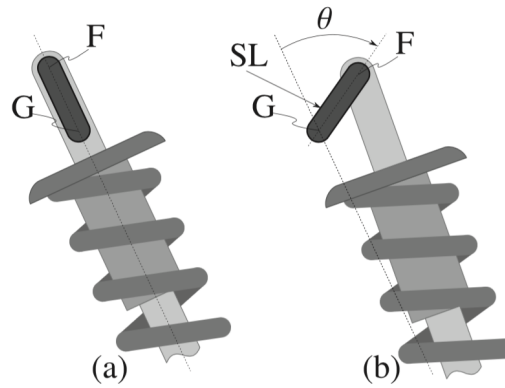


Figure 2.1: Simplest version of SAVGS. (a) and (b) are different configurations that can be achieved by applying torque about G [12]

Figure 2.1 shows a single link (SL) that has been fitted between the top of the spring damper unit (SD). The length and orientation of the entire suspension unit and thus ratio of wheel to spring movement, or installation ratio, can be adjusted by rotating and changing the angle of the SL, referred to as θ . This rotational link introduces a geometric non-linearity which poses a problem for traditional linear control techniques.

One of the main advantages of SAVGS is in its integration of the concept of variable geometry suspension where energy expenditure is reduced by applying actuation forces at right angles to the main suspension forces[13]. This is used in conjunction with more common active suspension concepts where the control actions of the suspension are directly applied to the main suspension forces [12], resulting in a significantly less power hungry alternative to traditional active suspensions.

SAVGS avoids another disadvantage found in the active suspension mentioned in section 2.3.2 by being able to operate in case of power or actuator failure, as the spring damper unit will still operate. Its active on demand capabilities also allow it to work with potentially zero power consumption when idle.

So far the SAVGS has only been tested on a GT car through simulations. When controlled with a Proportional Integral Derivative (PID) controller [14][15] it performed promisingly with respect to low frequency disturbances such as body roll during cornering. Robust linear control methods have also been tested in an attempt to increase the bandwidth of the suspension. Work is still ongoing to optimise the control scheme, but recent progress has shown promising results [12][16].

2.4 Road Disturbances and Sensitivity on the Human Body

In order to effectively evaluate the needs of a suspension system, it is of interest to understand the type of disturbances that will affect a car on the road, and how they affect the passenger.

2.4.1 Road Quality Classification

Measurements published in 1936 [17] stated that in terms of inches of irregularities per mile of road in the UK, the index for the best roads were found to be 75-85 in/mi (inches per mile), whereas for main roads the indices ranged from 100 to 250 in/mi. There is little evidence to suggest that these figures have changed significantly over the years.

These reports give a rough indication on the typical condition of certain types of roads, but do not give any indication as to whether the irregularities are caused by a few large irregularities or several smaller ones. It is therefore not particularly useful for input in a simulation. Survey work from the 1970s [18] that presents the results of roughness of roads as vertical displacement power spectral density (PSD) in units of feet against spatial frequency in units of cycles per feet, is preferred. This method allows a computer model to artificially generate a signal conditioned to have the same PSD as the road on which one wishes to test the car. The International Organisation for Standardisation (ISO) has classified good, average and poor roads based on their spectral profile, as seen in Figure 2.2.

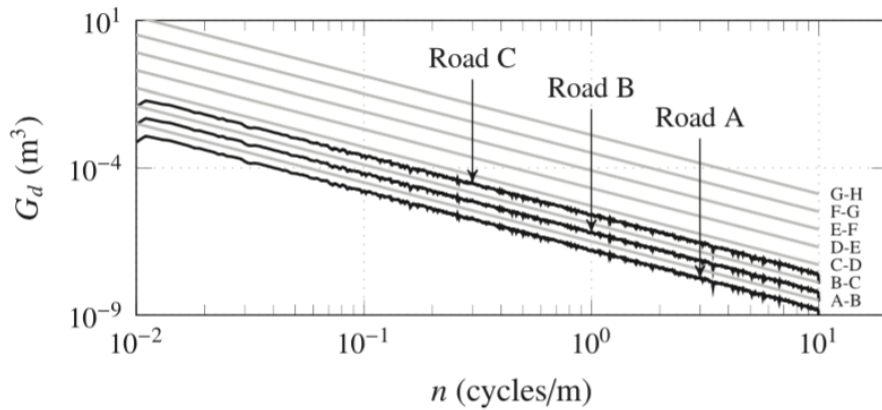


Figure 2.2: Displacement of power spectral density, G_d , as a function of spatial frequency n . [12]. Roads A, B and C are considered good, average and poor roads [19]

2.4.2 Human Sensitivity to Vibration

Vibrations of different frequencies disturb the human body in different ways. Vertical vibrations in the frequency range of 4-8Hz cause whole body vibration, whereas vibrations in the frequency

range of 18-200Hz only affect certain parts of the body. For example, the head with respect to shoulders within 18-30Hz, and lower jaw with respect to head at 100-200Hz. Vertical vibrations in the range of 0.5Hz and 0.75Hz affect spatial orientation causing motion sickness [1]. It is therefore imperative that the control synthesis be weighted towards minimising vibrations within the range of critical frequencies.

2.4.3 Performance Metrics for Road Isolation and Road Holding

To quantitatively assess the ride comfort, the Ride Comfort Index (RCI) as proposed by the ISO will be used [19]:

$$RCI = \sqrt{\frac{1}{T} \int_0^T \ddot{z}_s^2(t) dt} \quad (2.1)$$

where T is the length of time over which the vibrations occur and \ddot{z}_s is the vertical sprung mass acceleration. This equation physically represents the root mean square (RMS) of the sprung mass acceleration. In addition to this, the ISO proposes a Ride Holding Index:

$$RHI = \sqrt{\frac{1}{T} \int_0^T \Delta l_t^2(t) dt} \quad (2.2)$$

where δl_t is the vertical tyre deflection. This equation represents the root mean square (RMS) value of the tyre deflection.

In addition to these techniques, the PSDs of the sprung mass acceleration and tyre deflections will be analysed. The power spectrum of a signal describes the distribution of power into frequency components composing that signal, and as such it enables a quantitative assessment of the performance of the suspension at different frequencies.

2.5 Car and Suspension Modelling

When modelling a car body, a quarter-car model is first be considered, and then extended to a full car model. This section introduces these concepts, as well as the non-linear multi-body model used to simulate the SAVGS when retrofitted onto a car.

2.5.1 Quarter Car Model Concept and Theory

The quarter-car model consists of one wheel with its corresponding suspension, and one quarter of the sprung mass. A mechanical linear model of a quarter car is shown in Figure 2.3.

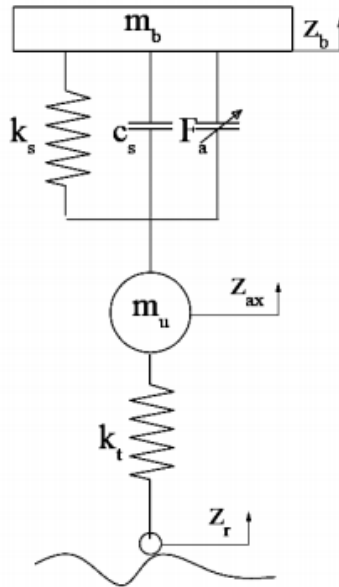


Figure 2.3: Quarter Car Mathematical Model [20]

This model assumes that the tyre can be modelled as a linear spring without damping (k_t), and that there is no rotational motion between wheel and body [21]. The limitations to the model are that it gives no representation of the geometric effects of the full car, or the longitudinal and lateral interconnections.

This model therefore has two degrees of freedom (DOF): the axle and body deflections (z_{ax} and z_b). This is a simplistic and qualitatively correct study for the vertical motion of the vehicle

and thus the handling and comfort of the quarter car can be studied from each of the DOFs respectively.

2.5.2 Half Car Model Concept and Theory

The half car model is constructed by combining two quarter car models, and is shown in Figure 2.4.

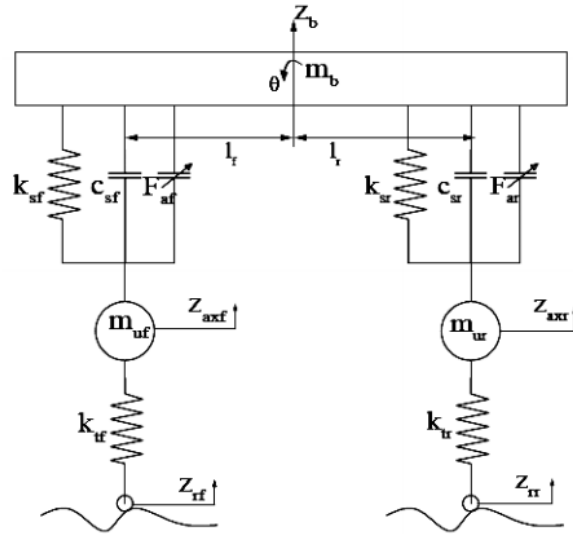


Figure 2.4: Half Car Mathematical Model [20]

This model has four degrees of freedom as in addition to the vertical deflection of the axle and body, the pitch and heave (θ and z in Figure 2.4) of the car can also be studied [21]. These are low-frequency disturbances which are already confirmed to be well controlled by the SAVGS and thus the half-car model will not be considered for the purposes of the project.

2.5.3 Full Car Model Concept and Theory

A full car model is constructed with four quarter car models attached to the corners of a rigid rectangular frame which models the chassis. This is shown in Figure 2.5.

The seven degrees of freedom in this model are Heave (z), pitch (θ), roll (ϕ), and the four vertical motions of all the axles (z_{axfR} , z_{axfL} , z_{axrR} , z_{axrL}) as in Figure 2.5[20]. Full car models of both

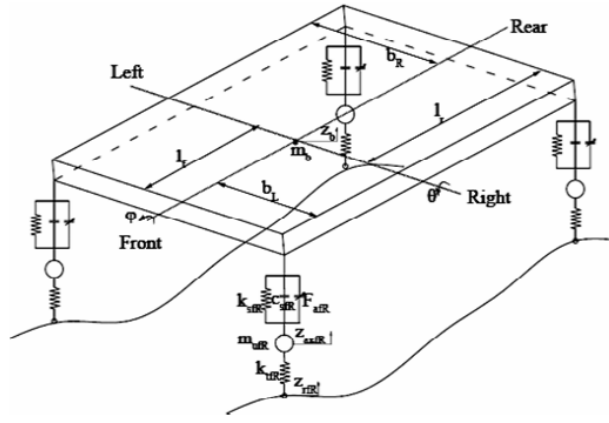


Figure 2.5: Full Car Mathematical Model [20]

the passive car and SAVGS enabled car will be synthesised in order to study the difference the SAVGS makes to the vertical motions of the car.

2.5.4 Multi-body Car Model for Simulation

To accurately simulate the non-linear dynamics of a car when it drives along a road, non-linear multi-body models will be synthesised for both the passive car and the car retrofitted with SAVGS in quarter and full car variations. These models are synthesised using AutoSim, a software described in section 2.7, in the form of Simulink compatible functions that specify the ordinary differential equations necessary to describe the car model's kinematical and dynamical behaviour. The number of equations will vary depending on the type of car model used. The behaviour of the car is then output by the model as signals that can be analysed and compared.

2.6 Controller Methodology Controller and Selection

Controller design is key in the successful implementation of the SAVGS. There are many different control methodologies used for active car suspensions but the three types of control methodologies that will be considered for this project are the PID, H_∞ and μ -synthesis methods. The latter two are Robust Linear Control methods.

2.6.1 PID Control

A PID control scheme is a control feedback mechanism that continuously calculates an error value $e(t)$ as the difference between a set point and a measured process variable. The scheme then applies a correction based on the proportional, integral and derivative of the error which physically correspond to the present, past and future error values respectively. The controller attempts to minimise the error over time by adjusting a control variable $u(t)$ as a weighted sum of the three terms [22]:

$$u(t) = K_p e(t) + K_i \int_0^t e(\tau) d\tau + K_d \frac{de(t)}{dt}$$

In the case of the SAVGS, the error term will be the error in the position of the single link [14].

The PID controller has previously shown good results for control of the SAVGS for low frequency disturbances such as body heave and pitch, but conclusive evidence has shown that the two alternative control techniques enable a higher bandwidth of control. As such, a PID controller for the sports car will not be investigated.

2.6.2 Robust Linear Control

Due to the rotating SL in the SAVGS, several non-linearities are introduced into the suspension model. Linearisation based on energy conservation principles [12] as explained in Section 3.3.1 allow robust linear control techniques to be used to control the rotation of the SL. Robust linear control is a control design methodology that takes uncertainties into account in its model. Uncertainties are differences or errors between the model and reality. The degree to which a controller is able to maintain its level of performance in light of uncertainties is called its robustness [22].

Two types of robust linear control techniques will be considered in this project: the H_∞ control scheme, whose application to SAVGS is well documented and proven to perform desirably,

and the μ -synthesis controller which is less explored. This is the control scheme that will be employed in this project.

2.6.3 H_∞ Control

The H_∞ controller takes its name from the mathematical space over which its optimisation takes place: the H_∞ space. This is the space of matrix-valued functions that are analytical and bounded in the open right half of the complex plane ($Re(s) > 0$)[22]. Much of the machinery of synthesising the controller can be circumvented by using the *hinfsyn* function in MATLAB.

This control methodology is well documented for the control of SAVGS and has been proven to synthesise a high bandwidth controller when applied to the GT car [12]. Thus it will be the control methodology used for experimentation on the MX5.

By taking different combinations of uncertainties in the car model into account, different variations of a H_∞ controller can be synthesised. These controller will vary in aggression, and a brute force approach must be taken to find the best performing combination of uncertainties. Due to time limitations, this endeavour will not be carried out and a standard model without uncertainties will be used to synthesise the controller.

2.6.4 μ -synthesis Control

The μ -synthesis control method is less well documented than the H_∞ controller, but previous literature has shown that it may outperform the H_∞ control scheme [22]. However, due to its complexities and the time limitations of this project, it will not be considered for use on this project [23].

2.7 Software

The three main software packages that will be used are MATLAB, Simulink and AutoSim.

MATLAB is a programming language developed by MathWorks intended primarily for numerical computing. It has many existing toolboxes that facilitate uses in subjects ranging from biology to economics, but the one most relevant for this project is the Control System Toolbox. This contains algorithms and applications for analysing and designing linear control systems. The linearised model will be used in conjunction with this toolbox to synthesise a controller for the SAVGS.

Simulink, also developed by MathWorks, is a graphical programming environment for simulation and model-based design that integrates with MATLAB. This software will be used to close the loop for the active suspension and ultimately run the car models to simulate its performance.

AutoSim is a software package that originated from the University of Michigan that "predicts the performance of vehicles in response to driver controls (steering, throttle, brakes, clutch, and shifting) in a given environment (road geometry, coefficients of friction, wind)" [24]. It will be used to synthesise the multi-body non-linear model to which the controller will be connected in a closed-loop.

2.8 Background Summary and Conclusions

This chapter covered technical details on the different types of car suspensions currently used in the motor industry, and introduced the concept of SAVGS. Additionally, performance requirements and evaluation techniques that will be utilised in the simulation and evaluation of the SAVGS were presented. The theory behind the modelling of a car suspension was also provided. Finally, the motivation behind the selection of the H_∞ controller was given, as well as the use of software that will be used to synthesise this controller, and also carry out the simulations.

Chapter 3

Sports Car Suspension Modelling

This chapter introduces the design of a linearised model of the SAVGS for the object of focus for this project, the Mazda MX5. This is the model that will be used for the closed loop control of the SAVGS. Contrasts in the car will be drawn with the the Ferrari F430, the GT car that was used in previously published SAVGS experiments. Due to the variations in the dimensions of the suspensions of the two cars, the functions used to linearise the model of the F430 must be modified to fit the MX5. These modifications are covered in this chapter. The linearised model enables the use of robust linear control techniques to be used to synthesise the controller. The physical parameters of the MX5 must be acquired, and so the acquisition process and values of these parameters are also reported.

3.1 Sports car vs GT car

According to the Merriam-Webster dictionary, a sports car is a "2-passenger car designed for quick response, easy manoeuvrability, and high-speed driving" [25]. These characteristics are usually achieved by making the car as light as possible.

GT cars, or Grand Tourers, are performance luxury vehicles which like sports cars are capable of high speed. They are also designed for long distance driving and therefore normally have more luxuries and space for luggage compared to a sports car, and are consequentially be heavier.

3.2 Motivation Behind Car Selection

The sports car chosen to be the subject of this project is the 1998-2005 Mazda MX5 mkII due to the following reasons.

Firstly, the SAVGS must be retro-fitted onto a car with an independent, passive suspension that does not vary camber angle when vertical movement is introduced. This rules out all cars with a MacPherson strut suspension. The MX5 features an independent double-wishbone suspension, and the SAVGS can be installed onto it as shown in Figure 3.1.

Secondly, the MX5 has spare space at the top of the strut tower, where the SAVGS can be installed. This is typically a premium in newer cars. In the case that there will still be insufficient space for the SAVGS to be installed, it is possible to install smaller, after-market struts.

Lastly, the MX5 is budget-friendly, costing roughly £2000 for a basic, mid-production model.

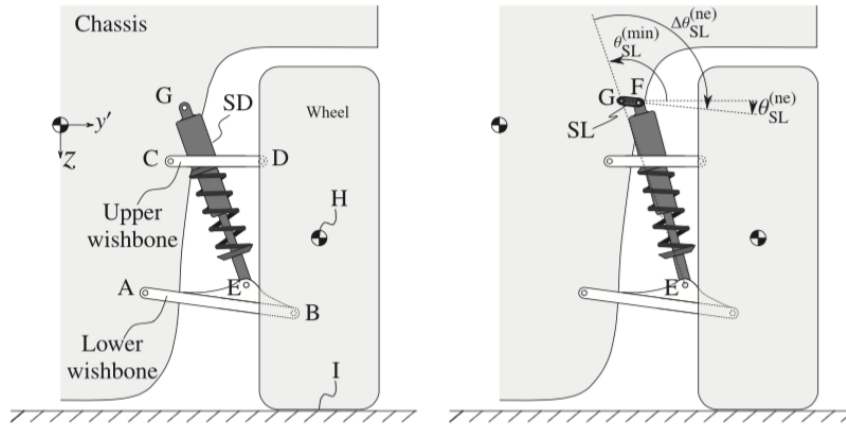


Figure 3.1: Left: Passive double-wishbone suspension. Right: SAVGS retrofitted double-wishbone suspension [1]

3.3 Simulation Model Modifications for the MX5

3.3.1 SAVGS Linearised Model

The main concepts of the SAVGS linearised model used for the MX5 are same as those used for the GT car, but some modifications must be made due to differences in the cars' parameters.

The main difficulties in modelling the SAVGS come from the non-linearities introduced by the rotating SL angle and actuator control [14]. The non-linear, multi-body models synthesised using AutoSim are appropriate for simulating the dynamical behaviour of the car body and thus the performance of the SAVGS, but are poor representations of the system for control synthesis. If a model without a major reliance on SL angle is used however, a controller suitable for a wide range of SL angles can be synthesised [12]. The proposed quarter car model is shown in Figure 3.2.

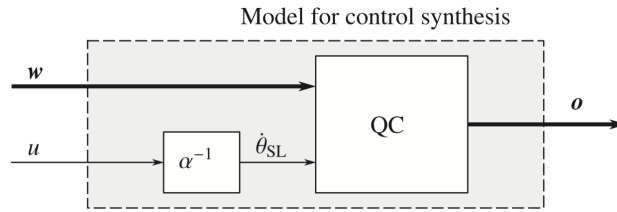


Figure 3.2: Linear model without strong dependency on SL angle [12]

The dependency on single link angle θ_{SL} is eliminated from the gains of the control input u to output o by using a new block α^{-1} , in which the non-linearity is lumped [12]. The chosen inputs and outputs of the system are documented in Section 4.2. A hand-derived model of the quarter car model with SAVGS can be constructed with consideration to Newton's Second law, and is shown in Figure 3.3. A glossary of its parameters is shown in Table 3.1.

Several important considerations must be made when modelling a multi-body quarter car to a linear one as shown in Figure 3.3. Firstly, it has been assumed that for the linear model, the sprung masses are fixed and the unsprung mass moves with the wishbone. This is to simplify the model.

Secondly, if the multi-body and linear quarter car model sprung masses, m_s and $m_s^{(eq)}$ respec-

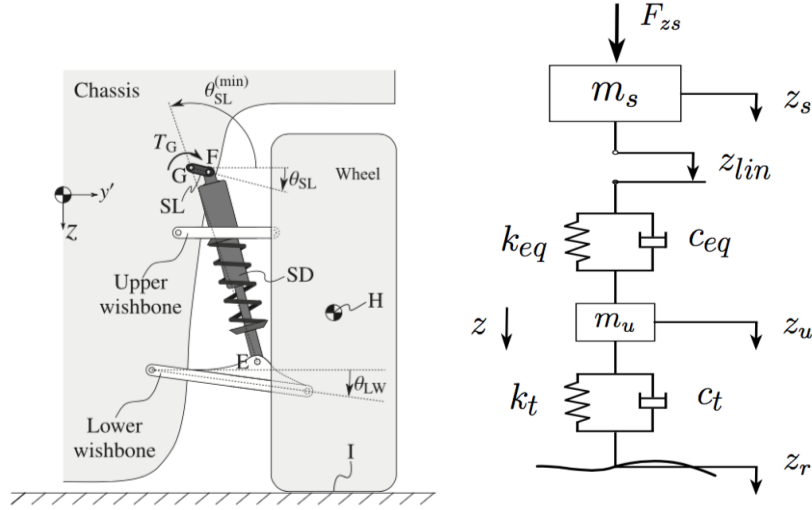


Figure 3.3: Left: SAVGS Retrofitted onto a double-wishbone suspension. Right: Hand-derived model [12]

Table 3.1: Hand Derived Model Parameters

| Parameter | Notation | Units |
|---|--------------------------|---------------|
| Sprung Mass Displacement | z_s | m |
| Unsprung Mass Displacement | z_u | m |
| Road Disturbance Displacement | z_r | m |
| Equivalent Suspension Stiffness | c_{eq} | $\frac{N}{m}$ |
| Equivalent Suspension damping coefficient | k_{eq} | $\frac{N}{m}$ |
| Suspension Deflection | $\Delta l_s = z_u - z_s$ | m |
| Tyre Deflection | $\Delta l_t = z_r - z_u$ | m |
| External Vertical Force | F_{zs} | N |
| Linear actuation displacement | c_t | $\frac{N}{m}$ |
| Deflection of the equivalent SD | $l_{SD}^{(eq)}$ | m |

tively only move vertically and in the same motion, an equality for the sprung displacements in each model, z_s and $z_s^{(eq)}$, can be drawn:

$$z_s^{(eq)}(t) = z_s(t)$$

Lastly, due to the series connection between the SL and passive SD, the suspension deflection is best expressed through a displacement input equal to the sum of the displacement of the equivalent linear actuator z_{lin} and equivalent SD deflection $l_{SD}^{(eq)}$ rather than a force/torque input [12]. Therefore:

$$l_s = z_{lin} + l_{SD}^{(eq)}$$

An expression for z_{lin} in relation to α can be derived by power considerations in the mapping between Figure 3.3 left, and Figure 3.3, right. This non-linearity can be expressed by a polynomial that is inversely proportional to the installation ratio, R_{SD} of the suspension, the ratio between the strut travel and wheel travel:

$$\alpha = -\frac{1}{R_{SD}} \frac{\partial l_{SD}}{\theta_{SL}} \quad (3.1)$$

The installation ratio, R_{SD} , is defined as in Equation 3.2.

$$R_{SD} = \frac{\partial l_{SD}}{\partial z_H} = \frac{\partial l_{SD}}{\partial \theta_{LW}} \frac{\partial \theta_{LW}}{\partial z_H} \quad (3.2)$$

As the installation ratio, SD length and SL length vary from car to car, the α function used for the GT car must be re-evaluated for the suspension geometry of the MX5. The scaled α function used for the front of the MX5 is shown in Figure 3.4. Suspension parameters for the front and rear of the MX5 can be found in Table 3.2 in section 3.4.

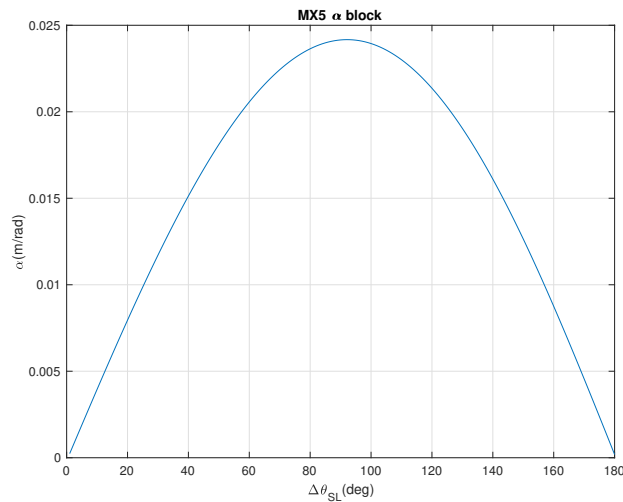


Figure 3.4: The evolution of α with single link angle for the front of the MX5

Additionally, the function β is introduced and is defined as the difference between the displacement of the equivalent linear actuator, and where the SAVGS is asked to operate by the controller, i.e. $z_{lin} - z_{lin(e)}$.

This function, like α , is dependent on the suspension geometry of the particular car in question. The β function used for the front of the MX5 is shown in Figure 3.5.

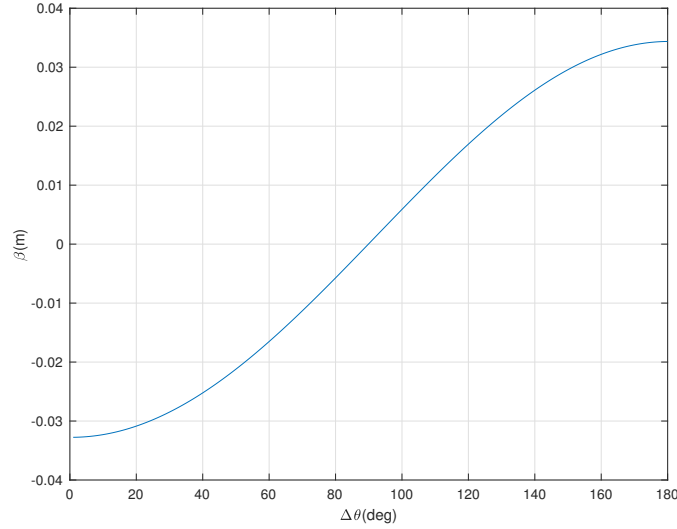


Figure 3.5: Evolution of β with single link angle for the front of MX5

Further material on the physics behind the equivalent model can be found in the following: [12], [14], [16].

3.3.2 SAVGS State Space Model

A state-space model is required to synthesise a controller for the SAVGS system. This is a mathematical model that provides a map from input to responses. The quality of the model is dependent on how accurately the responses of the model reflects that of the true plant, in this case a car. The differences or errors between model and reality are referred to as uncertainties.

The quarter car suspension system is a linear, MIMO system described by a state-space with representation [23]:

$$\dot{\mathbf{x}} = A\mathbf{x} + B\mathbf{u}$$

$$\mathbf{y} = C\mathbf{x} + D\mathbf{u}$$

where \mathbf{x} is the state variable vector, \mathbf{u} is the input vector, \mathbf{y} the output, and A, B, C and D are matrices of coefficients.

Defining the state variable vector, input and output as [23]:

$$\mathbf{x}^\top = \begin{bmatrix} \dot{z}_s & \dot{z}_u & \Delta l_s & \Delta l_t & z_{lin} \end{bmatrix} \quad (3.3)$$

$$\mathbf{u}^\top = \begin{bmatrix} \dot{z}_r & \dot{z}_{lin} & F_{zs} \end{bmatrix} \quad (3.4)$$

$$\mathbf{y}^\top = \begin{bmatrix} z_{lin} & \Delta l_t & \Delta l_s & \Delta \dot{l}_s & \ddot{z}_s & \ddot{z}_u \end{bmatrix} \quad (3.5)$$

The matrices of coefficients are therefore synthesised as [23]:

$$\mathbf{A} = \begin{bmatrix} -\frac{c_{eq}}{m_s} & \frac{c_{eq}}{m_s} & \frac{k_{eq}}{m_s} & 0 & -\frac{k_{eq}}{m_s} \\ \frac{c_{eq}}{m_u} & -\frac{c_{eq}+c_t}{m_u} & -\frac{k_{eq}}{m_u} & \frac{k_t}{m_u} & \frac{k_{eq}}{m_u} \\ -1 & 1 & 0 & 0 & 0 \\ 0 & -1 & 0 & 0 & 0 \\ 0 & 0 & 0 & 0 & 0 \end{bmatrix} \quad (3.6)$$

$$\mathbf{B} = \begin{bmatrix} 0 & -\frac{c_{eq}}{m_s} & \frac{1}{m_s} \\ \frac{c_t}{m_u} & -\frac{c_{eq}}{m_u} & 0 \\ 0 & 0 & 0 \\ 1 & 0 & 0 \\ 0 & 1 & 0 \end{bmatrix} \quad (3.7)$$

$$\mathbf{C} = \begin{bmatrix} 0 & 0 & 0 & 0 & 1 \\ 0 & 0 & 0 & 1 & 0 \\ 0 & 0 & 1 & 0 & 0 \\ -1 & 1 & 0 & 0 & 0 \\ -\frac{c_{eq}}{m_s} & \frac{c_{eq}}{m_s} & \frac{k_{eq}}{m_s} & 0 & -\frac{k_{eq}}{m_s} \\ \frac{c_{eq}}{m_u} & -\frac{c_{eq}+c_t}{m_u} & -\frac{k_{eq}}{m_u} & \frac{k_t}{m_u} & \frac{k_{eq}}{m_u} \end{bmatrix} \quad (3.8)$$

$$\mathbf{D} = \begin{bmatrix} 0 & 0 & 0 \\ 0 & 0 & 0 \\ 0 & 0 & 0 \\ 0 & 0 & 0 \\ 0 & -\frac{c_{eq}}{m_s} & \frac{1}{m_s} \\ 0 & 0 & 0 \end{bmatrix} \quad (3.9)$$

The equivalent stiffnesses of the springs, k_{eq} , and equivalent damping coefficients on the dampers, c_{eq} , can be calculated by considering that for the real and equivalent models, an equality must hold for the rate of change of energy stored in the springs and rate of change of energy dissipation in the dampers [12]:

$$k_{eq} = kR_{SD}^2 - F_{SD} \frac{\partial R_{SD}}{\partial z_H} \quad (3.10)$$

$$c_{eq} = cR_{SD}^2 \quad (3.11)$$

As evident from Equations 3.10 and 3.11, the equivalent stiffnesses of the springs and equivalent damping coefficients of the dampers depend on the angle of the single link, θ_{SL} and the angle of the lower wishbone, θ_{LW} . These hold only for when θ_{SL} and θ_{LW} are at their nominal values, stated in Equations 3.12 and 3.13

$$\theta_{SL}^{(ne)} = \theta_{SL}^{(se)} + \frac{\pi}{2} \quad (3.12)$$

$$\theta_{LW}^{(ne)} = \theta_{LW}^{(se)} \quad (3.13)$$

where the (ne) and (se) refer to the static equilibrium and nominal states respectively. The damping and spring coefficients are therefore nominally:

$$k_{eq}^{(ne)} = k_{eq}(\theta_{SL} = \theta_{SL}^{(ne)}, \theta_{LW} = \theta_{LW}^{(ne)}) \quad (3.14)$$

$$c_{eq}^{(ne)} = c_{eq}(\theta_{SL} = \theta_{SL}^{(ne)}, \theta_{LW} = \theta_{LW}^{(ne)}) \quad (3.15)$$

The nominal coefficients presented in equations 3.14 and 3.15 are substituted into the state space matrices 3.6, 3.7, 3.8, and 3.9 in order to realise the nominal state space.

As this state-space is only for the quarter car model, the synthesised controller will control whichever particular corner of the car the parameter values were chosen for. When the full car is to be simulated, a controller will be synthesised for each corner of the car using its corresponding parameter values. In total, four controllers will be synthesised and applied to each corner of the full car.

3.4 MX5 Physical Parameters

The parameters required to adequately model the suspension for control synthesis include chassis and suspension dimensions. The parameters required for the state-space model are listed in Table 3.2:

As first hand measurements of the car parameters cannot be taken and are unavailable from

Table 3.2: MX5 Parameters

| Parameter | Symbol | Unit | Value |
|---------------------------|------------|-----------------|--------------------|
| Quarter Car Sprung Mass | m_s | kg | 231.4 |
| Quarter Car Unsprung Mass | m_u | kg | 34.6 |
| Front Spring Stiffness | $k_{sd,f}$ | $\frac{N}{m}$ | 28370.5 |
| Rear Spring Stiffness | $k_{sd,r}$ | $\frac{N}{m}$ | 20665 |
| Damper Coefficient | c_{sd} | $\frac{N}{m/s}$ | 6000 |
| Tyre Radial Stiffness | k_t | $\frac{N}{m}$ | 2.42×10^5 |
| Tyre Damping Coefficient | c_t | $\frac{N}{m/s}$ | 300 |
| Installation Ratio Front | R_{SD} | n/a | 0.72 |
| Installation Ratio Rear | R_{SD} | n/a | 0.88 |

the car manufacturer, they must be estimated. The methods and/or justifications for the way in which the estimations were made are listed below:

- The quarter car sprung and unsprung masses were calculated by assuming a 50:50 weight distribution from the front to the rear of the car and taking a quarter of the curb weight (total weight, 1065kg), and assuming that the sprung to unsprung mass ratio is 6.69:1 (unsprung mass is 13% of curb weight), as suggested by [26].
- Front and rear spring stiffnesses are actual spring stiffnesses, not equivalent. Found from credible online sources [27].
- The damper coefficient is an estimation from credible online sources [28].
- As the tyre is modelled as a gas spring, it is estimated that 90% of its stiffness comes from inflation pressure [29] with the rest dictated by the thickness and make-up of the tyre compound. As the radial stiffness of the tyres of the F430 is known ($2.75 \times 10^5 \frac{N}{m}$), and the recommended inflations for the tyres of each car are known (33psi for the F430 and 29psi for the MX5), the stiffness of the MX5 tyres are taken as a direction proportion ($\frac{29}{33} \approx 0.8788$) of the F430's, as a fraction of their tyre pressures. This is an acceptable assumption as the gas in gas springs apply constant pressure, and pressure is directly proportional to force.
- The damping coefficient of a tyre is typically between 300 to 600 $\frac{N}{m/s}$. Is acceptable to claim that the tyre damping coefficient is small enough compared to the dampers that

precision is not a major factor, and so the lower estimate will be used, as this is what was used in the GT car model [30].

- The installation ratio is a measurement found from online sources [31].

This data is either gathered from the internet or estimated, rather than obtained through first hand measurements, and should therefore be used with caution.

By comparing these values to those of the F430, we see that there is a major difference in curb mass, with the MX5 weighing 1065kg and the F430 1440kg. In addition to this, the unsprung mass of the MX5 is significantly lower, which is especially beneficial for the road holding capabilities of the car. One parameter that seems suspect when the two cars are compared is the spring stiffness. The rear spring stiffness of the F430 is $157614 \frac{N}{m}$, over 7 times higher than that of the MX5. However, this is compensated by the higher installation ratio of the MX5. A measurement that is more indicative of the characteristics of a car's suspension is its spring rate which is proportional to the square of the installation ratio and inversely proportional to spring stiffness. For these two cars, the spring rate differs only by a factor of two. From these figures it can be expected that when driven in the same conditions, the MX5 will be more comfortable than the F430, but will experience higher tyre deflection.

It should be noted that the parameters for the front and rear of the car are different and therefore different controllers must be synthesised to control the different sides. Two of each car will be used to control the SAVGS at each corner of the full car.

When considering the full car, there are many other factors that may affect that MX5's suspension performance other than those listed. For example, the centre of gravity greatly affects the stability of the car when turning at high speed. Additionally the weight distribution between the front and rear of the car affect dive and squat severity. The aerodynamics and down-force generated by the body of the car will also be taken into account.

3.5 Chapter Summary and Conclusions

This chapter modified the α and β functions used to linearise the model of the SAVGS by considering the difference in suspension dimensions of the MX5 and F430. The parameters of the MX5 were also acquired, but some crucial parameters such as equivalent tyre stiffness had to be calculated. Arguments were made for the validity of these calculated values and were justified using scientific citations.

Chapter 4

SAVGS and Controller Design for the MX5

This chapter covers the decisions behind the design of the mechanical elements of the SAVGS and controller for the MX5. Most crucially, the length of the single link must be chosen to be long enough to allow an adequate range of control of the car's suspension characteristics, and a gearbox with a torque rating high enough to safely control the SL must be chosen. Additionally, this chapter documents the controller design and performance targets for the sports car SAVGS.

4.1 SAVGS Mechanics

4.1.1 Single Link Motor and Gearbox

The upper and lower limits of the SL angle are 0° and 180° . The SL is intuitively set to a nominal angle of 90° , allowing maximum movement in case of bumps or pot holes [1]. Results from [6] confirm that this provides the best attitude control performance.

The SL is rotated by use of an actuator fixed to the chassis, which comprises a servo motor and epicyclic gearbox. A servo motor can be either a rotary or linear actuator that consists

typically of a DC motor coupled with a sensor for position feedback, allowing for precise control over velocity [32]. An epicyclic gearbox consists of two gears, one which revolves in the centre of another and in comparison to other gearbox constructions have the benefit of being lower in weight and size [33]. Compactness is essential when the SAVGS is to be retrofitted, as typically car manufacturers do not leave much empty space near the suspension for extra components to be installed. If there is insufficient space in the MX5, a smaller after-market coil spring can be installed. The standard MX5 coil springs have diameter 3.27 inches and after-market coil spring can be found in 2.25 inch diameter variations.

The continuous torque requirements of the motor and gearbox will be determined by the length of the SL that will be explored in Section 4.1.2. An adequate margin should be left between the maximum required torque from the SAVGS and the maximum rated torque of the motor and gearbox as operating at maximum torque may overload the inverter if too much current is drawn.

4.1.2 Single Link Length Considerations for the MX5

The length of the SL needs to be varied depending on the stiffness of the suspension. This is due to the fact that for a stiffer spring, less displacement in compression or extension is required for a given tyre force increment, and thus a shorter link can be used. The tyre force increment is defined by $F_{tz} - F_{tz}^{(ne)}$. Since the MX5 has relatively soft springs, a longer SL must be used.

The SL lengths used in the F430 were 15mm and 11mm in the front and rear respectively. By comparing the spring stiffness and installation ratios of the MX5 given in Section 3.4 and those of the F430 from previous studies [12], it can be theorised that the SL length that gives the best results for the MX5 using its original springs would be around 26.5mm and 30mm for the front and rear of the car respectively. At maximum SL offset, these provide 40% and 37% maximum tyre force increments. These are the values that will be used in the simulation.

Approximately 111Nm SAVGS torque would be applied to the both the front and the rear single links to provide maximum SL offset.

Graphs of SAVGS torque against vertical tyre force increments for the front and rear suspensions with varying SL arm lengths are shown in Figures 4.1 and 4.2 respectively.

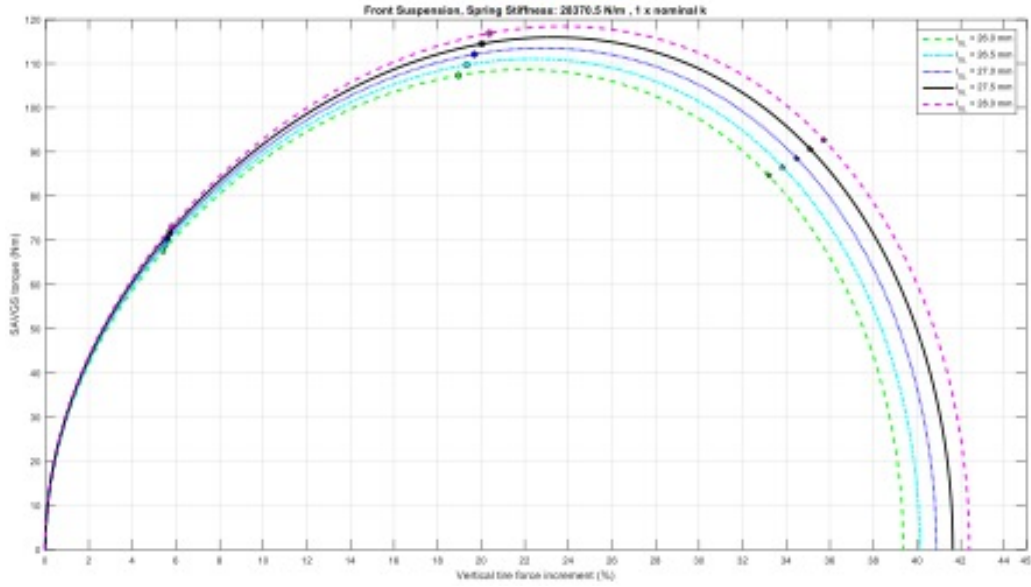


Figure 4.1: Graph of SAVGS torque against vertical tyre force increment for different SL arm lengths options for the front wheel with standard spring stiffness [34]

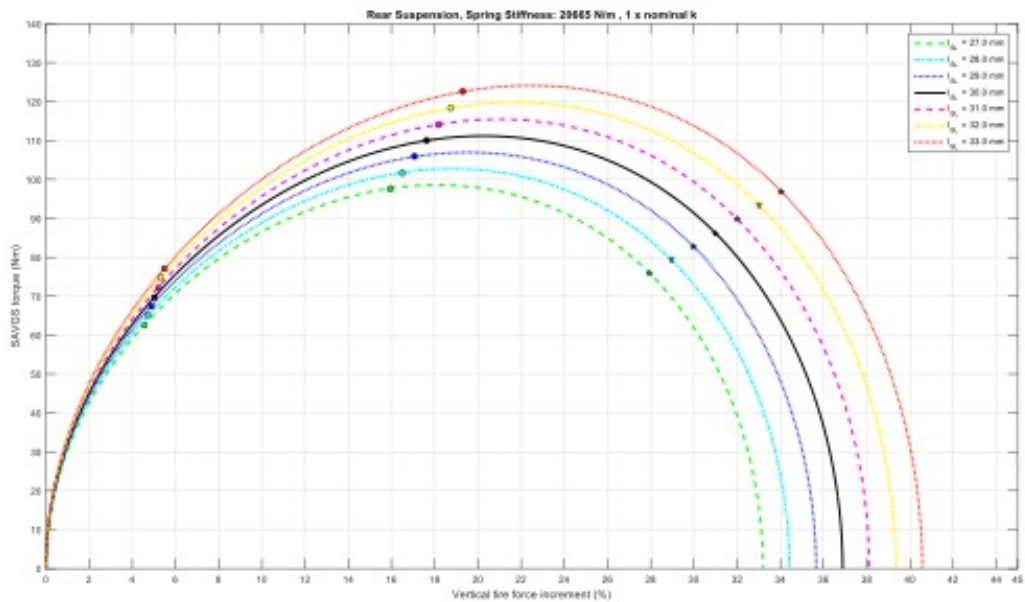


Figure 4.2: Graph of SAVGS torque against vertical tyre force increment for different SL arm lengths options for the rear wheel with standard spring stiffness [34]

4.2 Controller Inputs and Outputs

The input and output signals available to the SAVGS must be understood in order to effectively synthesise a controller.

4.2.1 Exogenous Disturbances, w

The three exogenous disturbances to be used for the SAVGS controller synthesis are the rate of change of road height, vertical load transfer, and exogenous position command of the single link.

Rate of change of road height, \dot{z}_r , is the most prominent of the three disturbances listed, and is caused by individual road bumps, pot holes, or general road unevenness.

Vertical load transfer, denoted by F_{zs} , is vehicle body acceleration that causes the vehicle body to stray from horizontal.

The position command of the single link is the command provided from higher level controllers, notated by $\theta_{SL}^{(e)}$ or $z_{lin}^{(e)}$ when using SL rotations or the displacement in the linearised model.

Measurement errors can be excluded as an exogenous disturbance as work has shown that sufficient robustness can be achieved without these signals [12].

The exogenous disturbances can be expressed as a matrix:

$$\tilde{\mathbf{w}}^\top = \begin{bmatrix} z_{lin}^{(e)} & \dot{z}_r & F_{zs} \end{bmatrix} \quad (4.1)$$

These values will be weighted during controller synthesis stages to either perform unit conversions or to scale the relative important of each signal. The weights are presented in Equation 4.5 in Section 4.3.

4.2.2 Control objectives and constraints, z

The two main objectives of the controller are to increase road isolation and road handling. In the context of a quarter-car model, the former is quantified by vertical acceleration of the sprung mass directly above the tyre and the latter by vertical tyre force variations or dynamic tyre deflections [12][19]. In the context of the full-car model, the acceleration of the sprung mass must be measured from the centre of gravity of the sprung mass which will be somewhere between the four wheels. The handling of the full-car is quantified by considering the tyre deflection of all four wheels.

Ride comfort and road handling are contrary to one another [35], and a balance appropriate for a sports car must be found. These objectives are achieved by applying the actuation torque on the SL to vary the geometry of the suspension, and the least amount of torque applied, and therefore energy expended, is desirable. Actuation torque and power cannot be realised in a linear model, and so the rotation and angular speed of the SL is penalised through z_{lin} and \dot{z}_{lin} respectively [12]. The controlled variables are therefore:

$$\tilde{\mathbf{z}}^\top = \begin{bmatrix} z_{lin}^{(e)} - z_{lin} & \ddot{z}_z & \Delta l_t & z_{lin} & \dot{z}_{lin} \end{bmatrix} \quad (4.2)$$

Again, these signals will be weighted, and the weights are presented in Equation 4.6 in Section 4.3.

4.2.3 Measurements, y

The signals available to the controller is dependent on the sensors. Two uniaxial accelerometers will be installed: one to measure vertical sprung mass acceleration, measured from the centre of gravity of the sprung mass, and the other for the vertical wheel acceleration, measured from the centre of the wheel. In addition to this, one linear variable differential transformer (LVDT) or potentiometer will be used to measure the suspension deflection, and one encoder will be used to measure the current angle of the SL [12]. The signals fed to the controller are therefore:

$$\mathbf{y}^\top = \begin{bmatrix} \Delta \dot{l}_s & \ddot{z}_u & \ddot{z}_s & z_{lin}^{(e)} - z_{lin} \end{bmatrix} \quad (4.3)$$

$\Delta \dot{l}_s$ is calculated by differentiating the measurement made by the LVDT.

During the controller synthesis stages, the term $z_{lin}^{(e)} - z_{lin}$ is multiplied by M , presented in Equation 4.7 in Section 4.3, and ensures that there is no steady-state error in the exogenous position command tracking [14][23].

4.2.4 Control action, u

There are two possible control outputs to be considered: equivalent SL speed and equivalent displacement. Equivalent SL speed is the preferred because it is required by the linear model to calculate damper forces and because it enables a simplified application of the control to circumstances where SL angle is not in its equilibrium state [12]. The control command is therefore:

$$u = \dot{z}_{lin}^* \quad (4.4)$$

However, this command control cannot be accurately tracked by the actuators at the wheels, and so a low-pass filter is introduced that can simulate the dynamic behaviour of the actuator [12].

4.3 System Interconnection

Robust control methods as introduced in Section 2.6.2 will be used to synthesised the controller used for the SAVGS. More specifically, the H_∞ control scheme as described in Section 2.6.3 will be used. The interconnection for the control synthesis is shown in Figure 4.3.

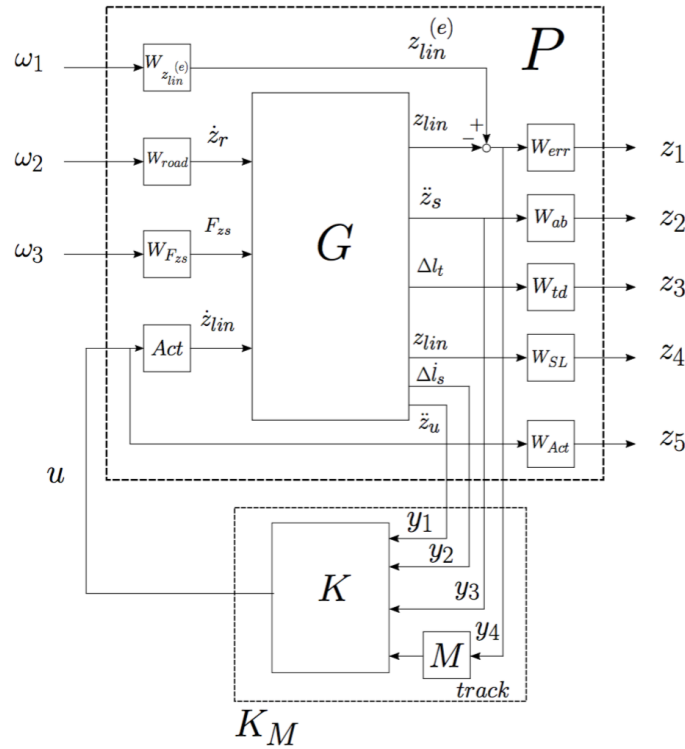


Figure 4.3: System interconnection [1]

The blocks labelled W are weights and are block diagonal matrices. One of their purposes is to perform unit conversion but the more critical purpose is to perform scaling on the relative criticality of each signal. Previous work has designed these weights based on the following performance criteria at each frequency range [12]:

- The tracking of the exogenous SL position command must be prioritised at low frequencies and negligible at high frequencies
- As humans are particularly sensitive to vibrations in the range of 1-10Hz, the sprung mass acceleration must be prioritised in this range
- Suspension and tyre deflection should be reduced in the 1-5Hz range
- The actuation effort should be concentrated below 10Hz

This criteria is based on theory presented in section 2.4.2 and is consistent across all cars and is therefore also used when considering the weights for the MX5. For an H_∞ controller however,

these weights must also be used to fulfil rank conditions and slight tuning had to be carried out in order to be able to synthesise a controller. The final weights used to synthesise the controllers are presented in Equations 4.5, 4.6 and 4.7.

$$W_{road} = 0.3, W_{F_{zs}} = 1000, W_{z_{lin}^{(e)}} = 0.02 \frac{1}{1 + \frac{s}{2\pi}} \quad (4.5)$$

$$\begin{aligned} W_{act} &= \frac{1}{0.1250} \frac{s + 50}{s + 500}, W_{ab} = \frac{1}{3} \frac{1}{1 + \frac{s}{2\pi 10}}, W_{sd} = \frac{1}{0.0225} \frac{1}{1 + \frac{s}{2\pi 5}} \\ W_{SL} &= 1, W_{td} = \frac{1}{0.075} \frac{1}{1 + \frac{s}{2\pi 5}}, W_{err} = \frac{1}{0.005} \frac{1 + \frac{s}{2\pi 150}}{1 + \frac{s}{2\pi 0.3}} \end{aligned} \quad (4.6)$$

$$M = \frac{1 + \frac{s}{2\pi}}{s} \quad (4.7)$$

The scalar weights and coefficients in these weights were determined by considering the expected maximum values of the signals. W_{err} is a pure integrator responsible for the exogenous SL position command tracking. W_{ab} , W_{sd} and W_{td} are first order low-pass filters with cut-off frequencies of 10Hz, 5Hz, and 5Hz respectively, that act on the sprung mass acceleration, suspension deflection and tyre deflection. W_{act} is a high-pass filter which penalises the high frequency components of the signal and thus limits the control bandwidth.

Comfort and handling targets are set by specifying closed-loop targets for the gain from road disturbance to body acceleration and suspension deflection respectively. The targets for the controllers used in the MX5 are displayed in Equation 4.8. Bode plots of these targets can be found in Figure 4.4.

$$\begin{aligned} \text{Comfort Target} &= \frac{1}{2} \frac{1}{1 + \frac{s}{2\pi 10}} \\ \text{Handling Target} &= \frac{1}{0.003} \frac{1}{1 + \frac{1}{2\pi 5}} \end{aligned} \quad (4.8)$$

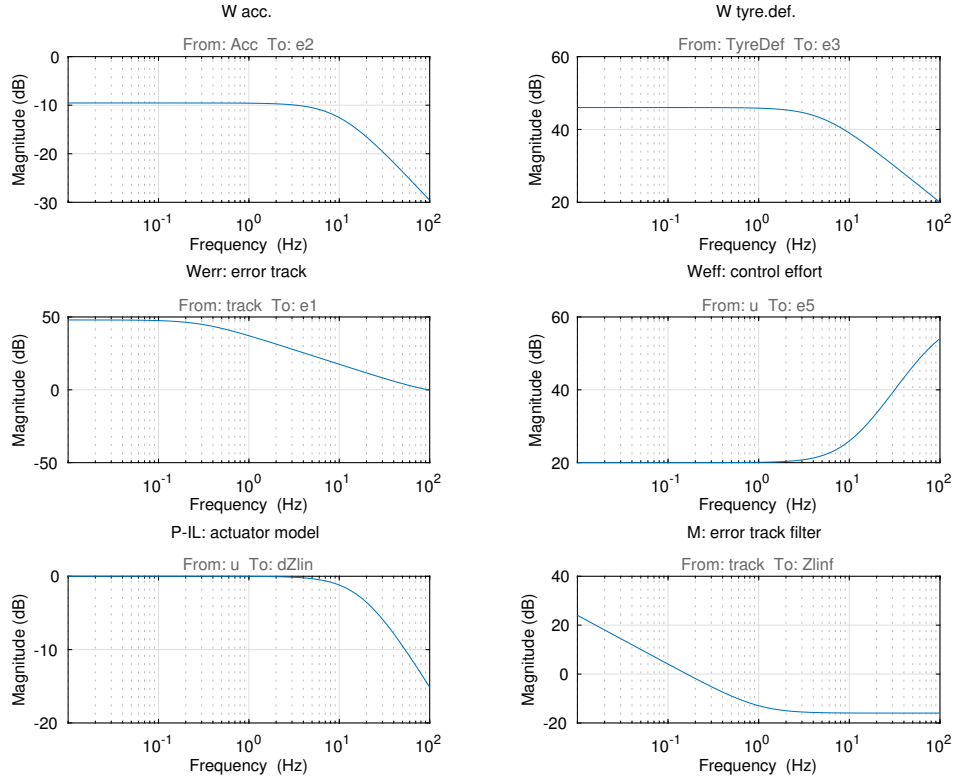


Figure 4.4: Bode plots of the comfort and handling targets

Despite the parameter differences, the selected weights satisfy the rank conditions necessary for controller synthesis for both the front and rear of the car, and will therefore be used for both. The comfort and handling targets are also consistent for all controllers synthesised for the MX5. The H_∞ controller is synthesised by specifying the interconnection in MATLAB and using the *hinfsyn* function.

4.4 Chapter Summary and Conclusions

The optimum SL lengths for the front and rear suspensions for the MX5 were identified in this chapter, and a minimum gearbox torque was suggested. The weights, comfort and handling targets used in the system interconnection used to synthesise the H_∞ controller were documented. These are crucial in shaping the characteristics of the controller and therefore play a key role in optimising the performance of the SAVGS.

Chapter 5

Simulation Results and Analysis

By utilising the non-linear, multi-body models and simulation techniques detailed in Chapter 2, the MX5's parameters and linearised SAVGS models documented in Chapter 3, and controller and SAVGS designs from Chapter 4, simulations of the sports car with both passive and SAVGS suspensions can now be carried out. This chapter analyses the performance of the quarter and full car models equipped with passive and active suspensions with respect to their road isolation and road holding abilities when subjected to roads with varying levels of disturbance severity.

5.1 Quarter Car Simulations

By using the parameters from 3.4 and interconnection from 4.3, a controller for the SAVGS can be synthesised using MATLAB. It is connected in a closed loop with the non-linear multi-body model synthesised on AutoSim within Simulink. This controller is dependent on the parameters of the car and may differ from the front to the rear of the car. This is the case for the MX5 and therefore the performance of the SAVGS when applied to the front and rear of the car will be analysed separately.

Simulations will be carried out on multiple different road conditions and disturbances in order to observe the results.

5.1.1 Quarter Car Simulation Results on a Single Bump

The initial test for the MX5 is the single bump expressed in the time domain by:

$$r(t) = \begin{cases} \frac{h}{2}(1 - \cos(2\pi\frac{V}{l}t)) & \text{for } 0 \leq t \leq \frac{2l}{V} \\ 0 & \text{for } t \geq \frac{2l}{V} \end{cases} \quad (5.1)$$

where h denotes the vertical displacement of the disturbance, V is the vehicle's forward velocity and l the longitudinal length of the bump. For the following test the height was chosen to be 5cm, the forward velocity to be 20km/h and the length of the bump to be 2.5m.

The exogenous position of the command is set to 90° with respect to the orientation of the strut tower, line \overline{EG} in 3.3.

A power efficient high bandwidth (10Hz) active car suspension passing over a minor road at 32km/h draws just over 1.5kW in power [36]. One of the motivations behind the SAVGS is to offer a high bandwidth active suspension solution that is less power demanding and so to ensure that this condition is met, a power limit of 1.5kW for the SAVGS was set.

In order to quantify the performance of the car, the Ride Comfort Index and Road Holding Index as introduced in 2.4.2. The sprung mass acceleration required for the RCI is measured from the centre of gravity of the sprung mass which will be directly above the wheel in question.

For a front quarter car, the sprung mass acceleration and tyre deflection against time are shown in Figure 5.1. The sprung mass acceleration of the passive MX5 is of a similar shape to that of the GT car, but of around half the amplitude. On the other hand the tyre deflection of the MX5 is worse. The settling time of the suspensions are almost exactly equal. This indicates that the MX5 is more comfortable than the F430, but has worse handling. This result was expected as the spring rate of the front wheel of the MX5 is around half of that of the GT's.

For the purposes of comfort and handling, lower sprung mass acceleration and tyre deflections result in better RCI and RHI values. It is therefore evident from these graphs that the signals

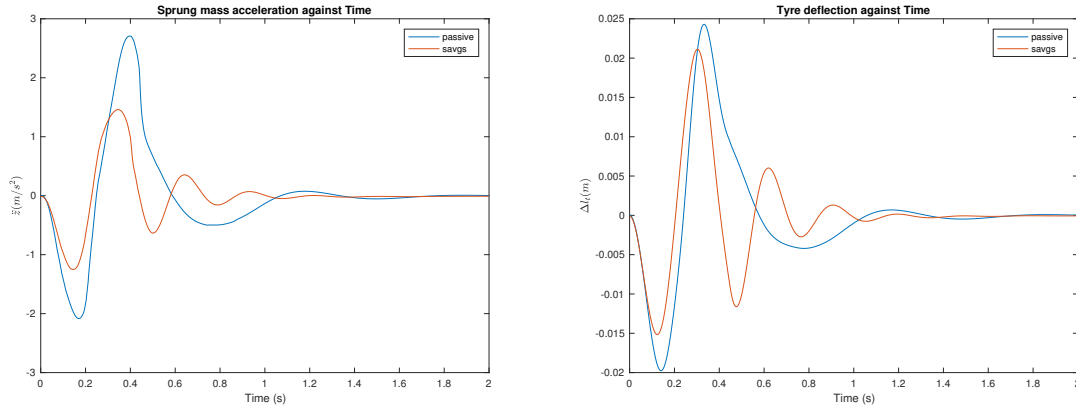


Figure 5.1: Left: Sprung mass acceleration. Right: Tyre deflection for front quarter car

obtained from the active case has a smaller maximum amplitude of the signal and therefore perform more desirably. Quantitatively, the RCI improved by 48.01% and the RHI by 22.67%. These values are not as large an improvement as those observed for the GT car, which were 63% and 61% respectively.

For the rear quarter car, the general suspension construction is different and vastly different results are yielded. The sprung mass acceleration and tyre deflection graphs for the rear quarter car are shown in Figure 5.2. Both of these signals differ in shape from that of the GT car and could signify that there is an error in the parameters used to simulate the MX5 rear quarter car. Therefore the following results should be treated with more care than those for the front quarter car.

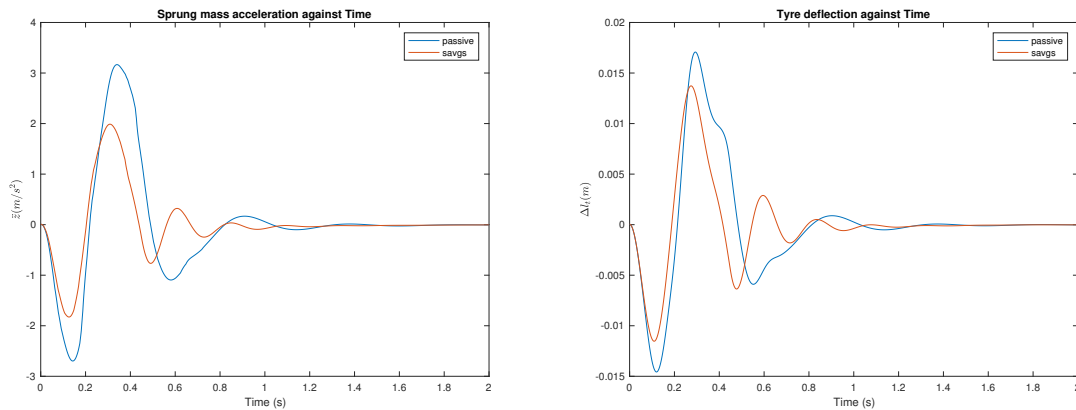


Figure 5.2: Left: Sprung mass acceleration. Right: Tyre deflection for rear quarter car

Again it is observed that the peak amplitude of the sprung mass acceleration and tyre deflection are reduced by the active suspension. When the RCI and RHI are evaluated, the SAVGS shows a 49.88% and 25.09% improvement respectively. In comparison to the F430, the same results are seen as the front quarter car: the suspension is more comfortable but provides less traction.

The improvements made by the SAVGS for the peak and RMS values of the relevant signals for both front and rear quarter cars are summarised in Table 5.1.

Table 5.1: Summary of improvements for quarter car on a bump

| Car Side | Parameter | Measure | Percentage Improvement (%) |
|----------|-----------|---------|----------------------------|
| Front | z_s | Peak | 35.52 |
| | | RMS | 48.01 |
| | t_d | Peak | 12.5 |
| | | RMS | 22.67 |
| Rear | z_s | Peak | 37.33 |
| | | RMS | 49.88 |
| | t_d | Peak | 18.78 |
| | | RMS | 25.09 |

When comparing the performance of the front and rear suspensions, the front suspension performs much more desirably than the rear suspension in both the passive and active cases, but the SAVGS results in a greater performance increase for the rear quarter car. When compared to the results from the F430 [12], it is observed that the comfort of the MX5 is indeed better than that of the F430, as theorised in Section 3.4. These results suggest that the SAVGS shows greater improvement when initial the passive suspension gives poorer results.

5.1.2 Quarter Car Simulation Results on a Random Road Profiles

Random road profiles of varying qualities were generated. The quality of the road profiles are quantified by their power spectral densities which can be approximated as follow [37]:

$$\Phi(\Omega) = \Phi(\Omega_0) \left(\frac{\Omega}{\Omega_0} \right)^{-\omega} \quad (5.2)$$

where $\Omega = \frac{2\pi}{L} \frac{rad}{m}$ denotes the spatial angular velocity, L is the wavelength, $n = \frac{\Omega}{2\pi}$ is the spatial frequency, $n_0 = 0.1 \frac{cycle}{m}$, and ω is the waviness, which for most road surfaces takes a value of 2. $\Phi(\Omega) = \Phi(\Omega_0)(\frac{\Omega}{\Omega_0})^{-\omega}$ is the amplitude of the power spectral density at the reference spatial angular velocity $\Omega_0 = 1 \frac{rad}{m}$. The severity of the disturbance that the vehicle is exposed to is determined in part by the velocity of the vehicle and in part by the roughness of the road. The one-sided power spectral density of the road profile is expressed as [37]:

$$\Phi(\omega) = \frac{\frac{\sigma^2}{\pi} \alpha V}{\omega^2 + \alpha^2 V^2} \quad (5.3)$$

where V is the vehicle's forward velocity and σ is the standard deviation of the roughness of the road. Table 5.2 summarises the standard deviation in parameters for different road classes.

Table 5.2: Summary of Road Class Values

| Road Class | $\sigma(10^{-3})$ | $\Phi(\Omega_0)(10^{-6}m^3), \Omega_0 = 1$ | $\alpha(rad/m)$ |
|------------|-------------------|--|-----------------|
| A | 2 | 1 | 0.127 |
| B | 4 | 4 | 0.127 |
| C | 8 | 16 | 0.127 |
| D | 16 | 64 | 0.127 |
| E | 32 | 256 | 0.127 |

Due to the purpose of the sports car, the car will be simulated on a race track with at road class A at a high speed. More specifically, the car will be simulated for a distance of 50m on a class A road travelling at 72km/h. RMS and PSD analysis will be carried out on the sprung mass accelerations and tyre deflections. The PSD is important as it will enable the gain at critical frequencies described in 2.4.2 to be analysed. These plots are shown in Figure 5.3 and Figure 5.4.

For the front quarter car, the main peak in the gain for the sprung mass acceleration in the front tyre is reduced slightly, but is increased for the tyre deflection. This is in line with the results obtained for the GT [12]. For the rear, the main peak is increased for both signals, albeit only very slightly for the sprung mass acceleration. This is undesirable. However, it can be pointed out that at lower frequencies, from 0Hz to 4Hz, the gain for all signals is reduced significantly. This suggests that the low frequency performance of the controller is very good. Additionally

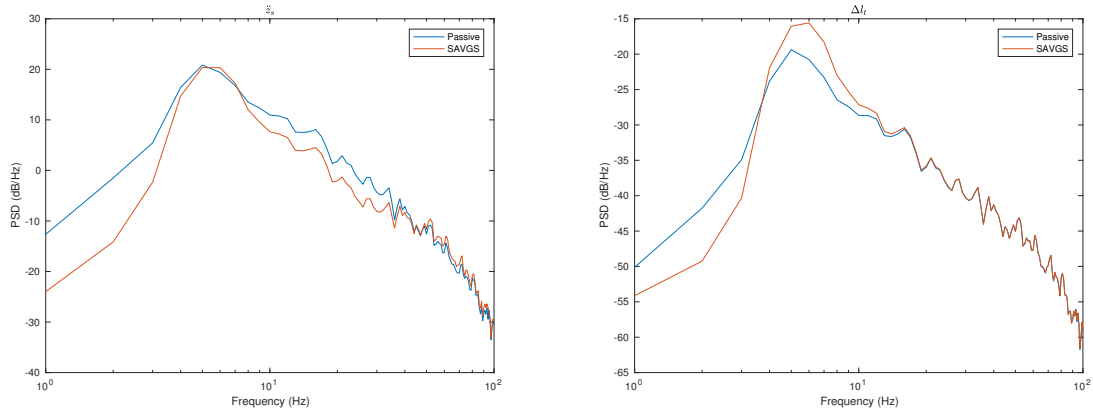


Figure 5.3: PSD of Left: Sprung mass acceleration. Right: Tyre deflection for front quarter car on a class A road

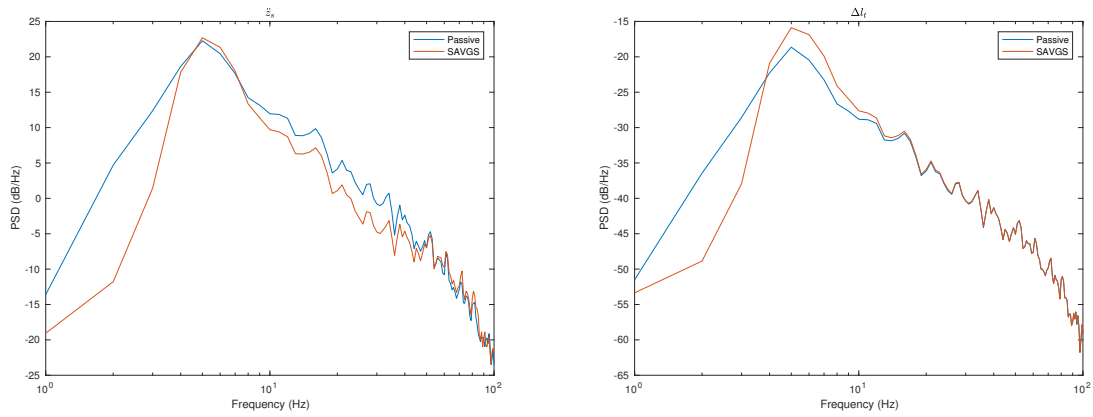


Figure 5.4: PSD of Left: Sprung mass acceleration. Right: Tyre deflection for rear quarter car on a class A road

for the sprung mass acceleration, the gain is reduced at frequencies between between 7Hz and 15Hz.

Altogether these results would indicate that the overall comfort of the vehicle is improved by the SAVGS. However, for the active suspension, vertical tyre forces are of a larger amplitude at the wheel hop frequency than for the passive suspension, which counter balances the improvements achieved at low frequencies. When the RMS values of the signals are analysed, it is found that overall, the handling has worsened. A summary of the results can be seen in Table 5.3

For the GT car, the SAVGS performed better on poorer roads. For example, the RHI was worsened by the SAVGS on a class A road but improved for a class C road. When the MX5 is

Table 5.3: Summary of improvements for Class A road

| Car Side | Parameter | Measure | Percentage Improvement (%) |
|----------|-----------|---------|----------------------------|
| Front | z_s | Peak | 11.90 |
| | | RMS | 10.39 |
| | t_d | Peak | -3.28 |
| | | RMS | -4.04 |
| Rear | z_s | Peak | 8.46 |
| | | RMS | 3.83 |
| | t_d | Peak | -8.34 |
| | | RMS | -8.12 |

tested on a class C road, the PSD plots for the front and rear quarter cars are as in Figures 5.5 and 5.6 respectively. For this poor quality road, the SAVGS significantly improves the wheel's tracking of the road. This is especially telling when the PSD plots are analysed, and it is observed that at lower frequencies, the SAVGS reduces the gain by almost 10dB.

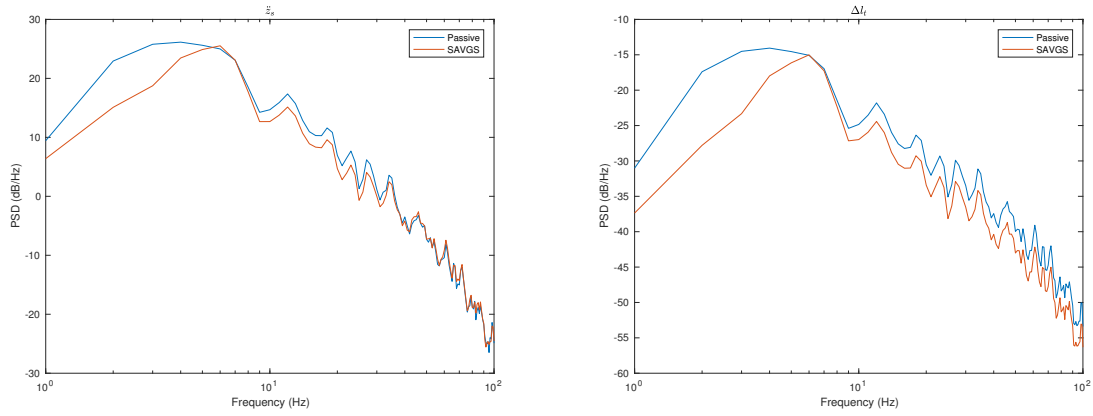


Figure 5.5: PSD of Left: Sprung mass acceleration. Right: Tyre deflection for front quarter car on a class C road

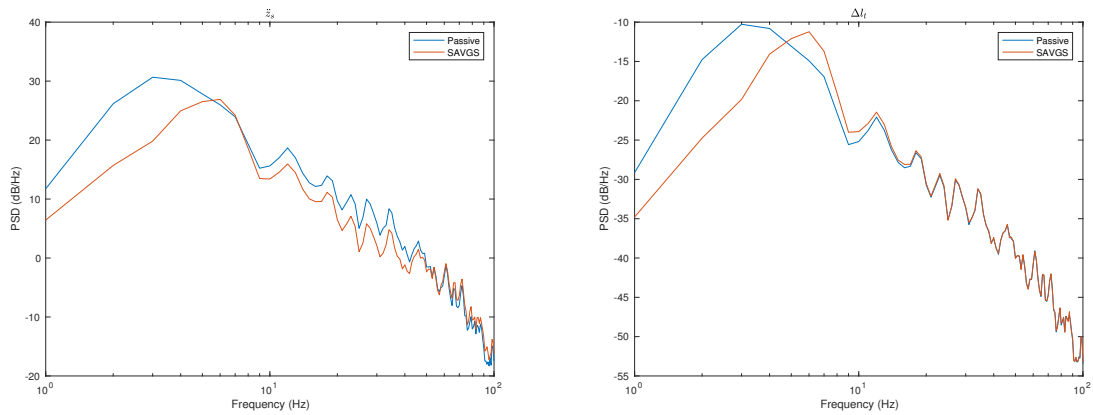


Figure 5.6: PSD of Left: Sprung mass acceleration. Right: Tyre deflection for rear quarter car on a class C road

Table 5.4 summarises the improvements made by the SAVGS.

Table 5.4: Summary of improvements for Class C road

| Car Side | Parameter | Measure | Percentage Improvement (%) |
|----------|-----------|---------|----------------------------|
| Front | z_s | Peak | 18.37 |
| | | RMS | 15.22 |
| | t_d | Peak | 10.65 |
| | | RMS | 11.04 |
| Rear | z_s | Peak | 16.13 |
| | | RMS | 17.92 |
| | t_d | Peak | 8.82 |
| | | RMS | 9.96 |

It should be highlighted that the SAVGS does not provide much comfort improvements at frequencies close the wheel hop frequency due to a zero in the transfer function from $\dot{\theta}_{SL}$ to vertical acceleration of sprung mass, \ddot{z}_s at that frequency. Similarly, the SAVGS does not reduce the suspension and tyre deflections at the rattle-space frequency [12]. This observation is corroborated by previous literature [38].

5.2 Full Car Simulations

The controllers synthesised for the front and rear car models are applied to the full car model and used to control the SAVGS in each corresponding corner.

As with the quarter car, the sprung mass acceleration is measured from the centre of gravity of the car model, but unlike the quarter car model, this point will not be directly above any of the wheels.

As the double wishbone suspension means each wheel is independent from the others, the road handling and tyre deflection will be measured in the same way as the quarter car.

5.2.1 Full Car Simulation Results on a Single Bump

The full car is driven over a single bump of height 5cm and length 2.5m at a speed of 20km/h. In this case the front wheels will traverse the bump first and then the rear wheels afterwards,

effectively causing the centre of gravity of the vehicle to experience two disturbances. The distance between the front and rear wheels is 3m and so the bump for the rear wheels is delayed by this amount. Plots of the sprung mass accelerations and the tyre deflection of the front left wheel are shown in Figure 5.7.

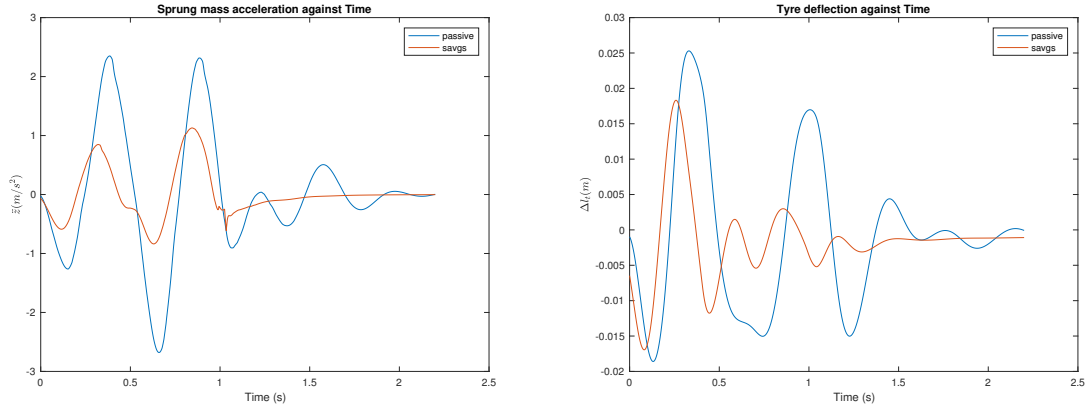


Figure 5.7: Left: Sprung mass acceleration of centre of gravity of full car. Right: Tyre deflection for front left tyre of full car.

Again, it can be seen that the SAVGS has reduced the peak values for both sprung mass acceleration and tyre deflection. The RCI was improved by 38.06% and the average RHI of all corners by 30.99%. Table 5.5 summarises the improvements.

Table 5.5: Summary of improvements for full car on a bump

| Parameter | measure | Percentage Improvement |
|-----------|---------|------------------------|
| z_s | Peak | 46.86 |
| | RMS | 38.06 |
| t_s | Peak | 35.07 |
| | RMS | 30.99 |

5.2.2 Full Car Simulation Results on Random Road Profiles

Random road profiles are generated for the full car in the same way as the quarter car, except different roads are generated for the left and right sides of the car. Again, the car is assumed to be driving in a straight line, so the rear wheels will be exposed to the same road profiles as the

front wheels, but delayed by 3m. Plots of the PSD of the sprung mass acceleration and tyre deflection when the car is driven on a 10km at 72km/h long class A road are shown in Figure 5.8.

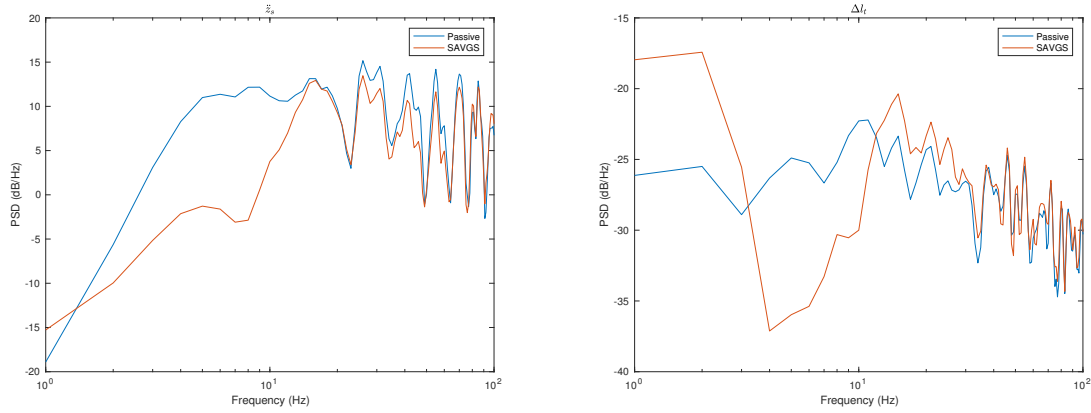


Figure 5.8: Left: PSD of Sprung mass acceleration of centre of gravity of full car. Right: PSD of average Tyre deflection of full car for a class A road.

With respect to the sprung mass acceleration, the gain for the SAVGS enabled car is below the passive car across almost all frequencies. For the tyre deflection, the SAVGS performs better at frequencies between 4Hz and 10Hz, but is significantly worse at frequencies between 1Hz and 3Hz. For much of this frequency range, the difference between the gains is over 5dB. The active suspension also performs slightly worse at the higher frequency ranges. Overall, it can be expected that much like the quarter car, the SAVGS decreases the road handling capabilities of the full car on good quality roads.

When the RMS values are evaluated, the RCI sees an improvement of 10.01% but the RHI is worse off by 6.13%. Further testing on other randomly generated class A roads showed similar results. It can therefore be concluded that in the case of the full car on a class A road, the SAVGS sacrifices the car's road handling ability for greater improvement in ride comfort. This trade-off can be seen as both beneficial or detrimental, depending on how the driver views the importance of each of these factors.

When tested on a class C road the following PSD plots in Figure 5.9 were obtained.

Again it can be seen that the SAVGS greatly improves the gain at frequencies below 10Hz for the sprung mass acceleration. At the 7Hz mark, the improvement is over 15dB. Small improvements

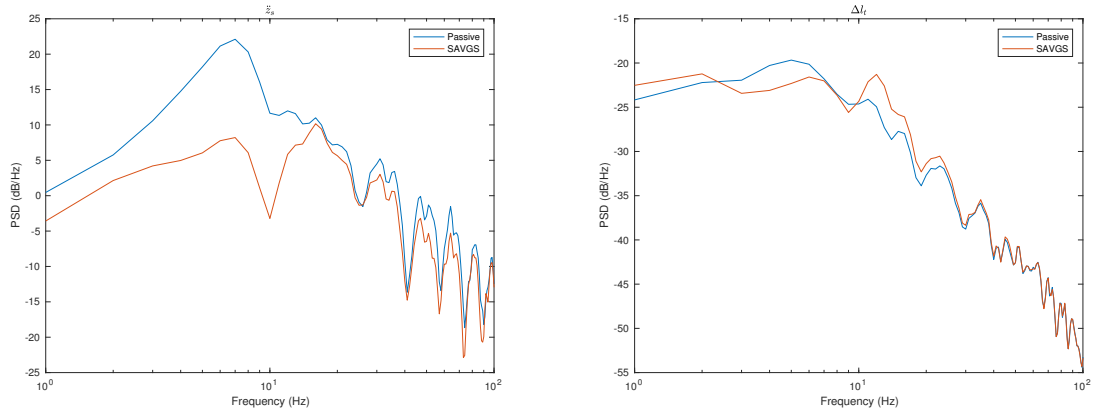


Figure 5.9: Left: PSD of Sprung mass acceleration of centre of gravity of full car. Right: PSD of Tyre deflection for front left tyre of full car for a class C road.

are also observed for frequencies above 10Hz. Much like the class A road therefore, these results suggest that the SAVGS improves the sprung mass acceleration of the car across all frequency ranges. In terms of tyre deflection, and in contrast to results seen for the class A road, the SAVGS and passive suspension have very similar gains across the observed frequency range. In the range of 1Hz to 11Hz, the difference in the gains never exceeds 5dB. When the RMS values are taken, it is found that the SAVGS improves the ride comfort by 8.56% and the road holding ability of the car is improved by 2.02%.

All code and data is available at [39].

5.3 Chapter Summary and Conclusions

By utilising the work covered in previous chapters, this chapter simulated the MX5 with both active and passive suspensions on variety of different road disturbances. These results were analysed by calculating the root mean squared values or power spectral densities of the sprung mass acceleration and tyre deflection signals and comparing the two suspensions. The analysis clearly demonstrates that SAVGS offers better road isolation than the stock suspension of the MX5 in all road conditions. Additionally, the road holding of the car is improved by the SAVGS when driven on average to poor roads. Given that this performance is achieved with a power limit set below that of a slow active suspension, it can also be concluded that the SAVGS is

less power demanding than typical active suspensions.

Chapter 6

Conclusions and Future Work

This project aimed to model a Mazda MX5 sports car and improve its performance in terms of comfort and handling by retrofitting a Series Active Variable Geometry Suspension. In the present research project, work has been carried out to obtain the physical parameters of the MX5 and to design a controller before the SAVGS performance was simulated and evaluated.

Many of the required parameters of the car are unavailable from first party sources such as the MX5's user handbook, and so estimations were made either using third party data from car owners or by carrying out informed calculations.

The controller synthesised was based on energy conservation principles derived for the GT car controller synthesis. By using exactly the same targets from the GT car for the MX5 results in a controller that is too conservative when comfort is evaluated. This may be due to the fact that the MX5 is more comfortable than the F430 to begin with. The controller synthesised for the MX5 was therefore made to be more aggressive.

The mechanics of the SAVGS also had to be changed to suit the MX5's softer suspension. It has been proven that in comparison to a stiffer spring, a softer suspension, a longer single link must be used to achieve a similar vertical tyre force increment.

The simulations in Chapter 5 show that in the case of a single bump, the SAVGS improves the performance of the suspension in terms of comfort and handling by almost 50% in certain

cases. This is less than the improvement observed in the GT car. It was also shown that for the quarter car on a good quality road, the SAVGS sacrificed road handling for comfort. These results are consistent with those of the GT car. On bad quality roads however, the SAVGS was shown to be extremely beneficial to both of the suspension's performance criteria. This pattern was also observed when the simulation was extended to a full car model.

A similar trend was observed when the simulations were extended to full car models. An improvement in comfort on the class A road was achieved in exchange for some road holding capabilities. On a class C road, the simulations indicated improvements in both metrics. These results suggest that the use of an appropriately controlled SAVGS improves the comfort and handling of the Mazda MX5 sports car over its stock suspension system, particularly in the case of bad quality roads.

6.1 Future Work

To further the accuracy of the simulation, more precise and reliable measurements for the MX5 can be acquired by taking first hand measurements. This may be an important next step given the uncertainty in some of the parameters used in this report.

Work has also been carried out on improving the SAVGS control. Another robust linear control technique, μ -synthesis control, has been investigated for the GT car in place of the H_∞ [20]. This particular piece of literature has also included analysis on the performance of different controllers synthesised with consideration to different combinations of uncertainties. A similar study can be carried out for the MX5, and other cars, and a comparison can ultimately be drawn to see if a particular combination of uncertainties is universally the best for all types of cars.

A different controller synthesis approach can also be taken by synthesising a controller for the full car itself, rather than synthesising a controller for the quarter car and then applying it to the full car. This is currently an ongoing project and is showing promise for improving both the comfort and handling of the full car in all road conditions. If successful, this approach should

also be taken to synthesise a controller for the MX5 to see if the results are consistent across different cars.

Bibliography

Front Cover Photo: T.W. White & Sons. (2013) Driven: classic Mazda MX5 review. [Online]. Available: <https://blog.twwhiteandsons.co.uk/car-reviews/mazda/classic-mazda-mx5-review/>

- [1] D. Bastow, G. Howard, and J. Whitehead, Car suspension and handling, 1993.
- [2] M. Abe and W. Manning, Vehicle Handling Dynamics: Theory and Applications, 1997.
- [3] W. Harris. (N/A) How car suspensions work. [Online]. Available: <http://auto.howstuffworks.com/car-suspension.htm>
- [4] Anonymous. (2010) Suspension basics 3 - leaf springs. [Online]. Available: <http://www.initialdave.com:80/cars/tech/suspensionbasics04.htm>
- [5] Anonymous. (2010) Suspension basics 4 - torsion bar springs. [Online]. Available: <http://www.initialdave.com:80/cars/tech/suspensionbasics03.htm>
- [6] A. Urugal and S. Fenster, Advanced Strength and Applied Elasticity, 2016.
- [7] M. Ansar and D. Unune, Active suspensions future trend of automotive suspensions, 2013.
- [8] S. Blanco. (2016) How does weight affect a vehicles efficiency? [Online]. Available: <http://www.autoblog.com/2009/10/29/greenlings-how-does-weight-affect-a-vehicles-efficiency/>
- [9] D. Sammier, O. Sename, and L. Dugard, Commande par placement de poles de suspensions automobiles, 2002.
- [10] K. Rujimon, M. Murtaza, and A. Krishnan, A comparison between passive and semi-active suspension systems, 2013.
- [11] R. Sharp and H. Peng, Vehicle dynamics applications of optimal control theory, 2011.

- [12] C. Arana, S. Evangelou, and D. Dini, Series active variable geometry suspension application to comfort enhancement, 2016.
- [13] R. Sharp, Variable active suspension for cars, 1998.
- [14] C. Arana, S. Evangelou, and D. Dini, Series active variable geometry suspension application to chassis attitude control, 2016.
- [15] Anonymous, Pitch angle reduction for cars under acceleration and braking by active variable geometry suspension, 2012.
- [16] C. Cheng, C. Arana, S. Evangelou, and D. Dini, Active variable geometry suspension robust control for improved vehicle ride comfort and road holding, 2015.
- [17] D. of Scientific and I. Research, Surface irregularities of roads, 1936.
- [18] R. L. Barre, R. Forbes, and S. Andrew, The measurement and analysis of road surface roughness, 1970.
- [19] International Organisation for Standardization (ISO), Mechanical Vibration and Shock: Evaluation of human exposure to whole body vibration, 1997.
- [20] K. Mahala, P. Gadkari, and A. Deb, Mathematical models for designing vehicles for ride comfort, 2009.
- [21] P. Sathiskumar, J. Jancirani, D. John, and S. Manikandan, Mathematical modelling and simulation quarter car vehicle suspension, 2014.
- [22] K. Zhou, J. Doyle, and K. Glover, Robust and Optimal Control. Prentice Hall, 1996.
- [23] A. Nazemi, Series active variable geometry suspension control, 2016.
- [24] M. Sayers, Symbolic computer language for multibody systems, 1992.
- [25] Merriam Webster Dictionary. (First Known Use: 1919) Sports car. [Online]. Available: <https://www.merriam-webster.com/dictionary/sports%20car>
- [26] R. Riley. (2016) Automobile ride, handling, and suspension design. [Online]. Available: <http://www.rqriley.com/suspensn.htm>
- [27] F. C. M. Inc. (N/A) Fcm elite coilovers for 90-05 miatas. [Online]. Available: http://fatcatmotorsports.com/FCM_Bilstein_coilover_revalve_NA_NB.htm
- [28] Anonymous. (2014) Damping to 65. [Online]. Available: <https://forum.miata.net/vb/archive/index.php/t548018.html>

- [29] Anonymous. (2012) Tyre vertical stiffness. [Online]. Available: <http://whitesmoke.wikifoundry.com/page/Tyre+vertical+stiffness>
- [30] Anonymous. (2010) Tyre vertical damping. [Online]. Available: <http://www.fltechnical.net/forum/viewtopic.php?t=16544>
- [31] Anonymous. (2011) Mx5 motion ratios? [Online]. Available: <https://forum.miata.net/vb/showthread.php?t=443709>
- [32] J. Zeiger and N. Nichols. (1942) Optimum settings for automatic controllers.
- [33] C. Kaim. (2000) The world of planetary gears. [Online]. Available: <http://www.machinedesign.com/motion-control/world-planetary-gears>
- [34] G. Cleaves, Single Link Length for SAVGS, 2017.
- [35] S. Türkiye and H. Akçay, Aspects of achievable performance for quarter-car active suspensions, 2008.
- [36] C. Pilbream and R.S. Sharp, Performance Potential and Power Consumption of Slow-Active Suspension Systems with Preview, 1996.
- [37] F. Tyan, Y.F Hong, R.O.C. and W.S. Jeng, Generation of random road profiles, 2009.
- [38] C. Yue, T. Butsuen, J.K. Hedrick, Alternative control laws for automotive active suspensions, 1988.
- [39] A. Zhou. (2017) SAVGS Code. [Online]. Available: <https://www.github.com/azhou95/SAVGS>